Journal of Porphyrins and Phthalocyanines
J. Porphyrins Phthalocyanines 2012; **16**: 761–784
DOI: 10.1142/S1088424612300091

Published at http://www.worldscinet.com/jpp/

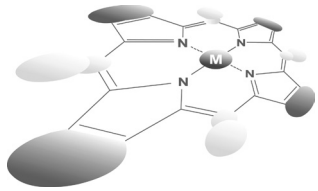

Oxygen reduction reaction using N_4-metallomacrocyclic catalysts: fundamentals on rational catalyst design

Justus Masa[a], Kenneth Ozoemena[b,c◊], Wolfgang Schuhmann[a] and José H. Zagal*[d]

[a] *Analytische Chemie — Elektroanalytik & Sensorik, Ruhr-Universität Bochum, Universitätsstr. 150, D-44780 Bochum, Germany*
[b] *Energy and Process Unit, Materials Science and Manufacturing, Council for Scientific and Industrial Research (CSIR), Pretoria 0001, South Africa*
[c] *Department of Chemistry, University of Pretoria, Pretoria 0002, South Africa*
[d] *Departamento de Química de los Materiales, Facultad de Química y Biología, Universidad de Santiago de Chile, Casilla 40, Correo 33, Santiago, Chile*

Dedicated to Professor Tebello Nyokong on the occasion of her 60th birthday

Received 7 March 2012
Accepted 24 April 2012

ABSTRACT: In this review, we describe and discuss the developments in the use of metalloporphyrins and metallophthalocyanines as catalysts for oxygen reduction in aqueous electrolytes. The main goal of most researchers in this field has been to design catalysts which can achieve facile reduction of oxygen by the four-electron transfer pathway at the lowest overpotential possible. With this in mind, the primary objective of this review was to bring to light the research frontiers uncovering important milestones towards the synthesis and design of promising N_4-metallomacrocyclic catalysts which accomplish the four-electron reduction of oxygen, and, based on literature, to draw attention to the fundamental requirements for synthesis of improved catalysts operating at low overpotentials. Our emphasis was not to make parallel comparisons between individual classes of N_4-metallomacrocyclic complexes with respect to their activity, but rather to focus on the commonalities of the fundamental properties that govern their reactivities and how these may be aptly manipulated to develop better catalysts. Therefore, besides discussion of the progress attained with regard to synthesis and design of catalysts with high selectivity towards four-electron reduction of O_2, a major part of the review highlights quantitative structure-activity relationships (QSAR) which govern the activity and stability of these complexes, which when well understood, refined and carefully implemented should constitute a fundamental gateway for rational design of better catalysts.

KEYWORDS: metalloporphyrins, metallophthalocyanines, N_4 macrocycles, oxygen reduction reaction.

INTRODUCTION

The electrochemical reduction of oxygen (ORR) is an important reaction in many electrochemical technologies including; fuel cells [1] chlor-alkali electrolysis, [2] metal-air batteries, [3] and electrochemical sensors [4] among others. In order to improve the overall efficiency of processes where this reaction is involved, suitable electrocatalysts have to be used. For example, platinum is the premium catalyst at both the anode and cathode of most low temperature fuel cells [5]. Significant improvements have been achieved regarding both the mass-specific and area-specific activities of platinum through its alloying with other metals, and through developments in synthesis of nanoparticles [6]. However, with the awareness that even the most ingenious improvements in catalyst synthesis cannot dispel the issue of platinum scarcity and

◊SPP full member in good standing

*Correspondence to: José H. Zagal, email: jose.zagal@usach.cl

cost escalation, it is a prudent endeavour to develop inexpensive catalysts for oxygen reduction reaction (ORR) which can be obtained from abundant and sustainable sources in order to realize the eagerly anticipated mass commercialization of fuel cells. For example, over the period from July 1st, 1992 to October 31st, 2011, records from Platinum Today, published by John Matthey, indicate that the world prices for platinum increased by an average value of $792.70 per troy oz [7]. The use of metallomacrocyclic complexes, particularly metalloporphyrins and metallophthalocyanines for ORR has been widely investigated since it was first reported in the 1960s that Co phthalocyanines catalyzed this reaction [8]. However, due to lack of systematic methodologies for prediction of macrocyclic complexes with desirable activity and stability, their performance with regard to both activity and stability generally trail those of catalysts derived from Pt. Of the metallomacrocyclic complexes that have been investigated for ORR, the N_4 metallomacrocyclic complexes, specifically metalloporphyrins and metallophthalocyanines, generally exhibit better activity compared to; N_2O_2 (Pfeiffer complexes), O_4, N_2S_2 and S_4 macrocyclic chelate complexes [9]. These materials are particularly interesting because of their lower costs compared to noble metals and their high tolerance to methanol, for the case of methanol fuel-cell applications. They are also interesting because they provide models where active centres can be identified, and their catalytic activity can be modulated by changing the structure of the macrocyclic ligand [10]. Several factors influence the activity and stability of metallomacrocyclic complexes for the oxygen reduction reaction (ORR). For a given macrocyclic ligand, ORR will vary with the type of central metal ion [11, 12]. Conversely, for a given metal ion, ORR will vary with the nature of substituents on the macrocyclic ligand [13, 14], due to the electronic density changes they induce on the metal ion. In addition to these inherent limitations, the ORR activity and stability of a given metallomacrocyclic complex is highly dependent on the pH of the electrolyte. This effect is more pronounced in acidic electrolytes than in alkaline ones [15]. The other factors which influence the activity and stability of a given metallomacrocyclic complex include; its solubility in a given electrolyte, the method of its immobilization on the electrode, the operating conditions, and whether the ORR is measured with the metallomacrocyclic complex in solution or adsorbed on an electrode [16]. The most commonly used methods for immobilization of metallomacrocyclic complexes on an electrode include: dip-coating, drop-dry, spin coating, electropolymerization, grafting, self-assembled layer(s), sublimation and spraying. As such, the ORR performance of a given metallomacrocyclic complex may also vary depending on the method of immobilization used. For example, it has been reported in some literature that the potential of the M(III)/M(II) redox couple and oxygen reduction are shifted to more positive values for films formed by electropolymerization compared to films formed by dip-coating or drop-coating. Therefore, because of the inevitable variations in experimental procedures and conditions from one laboratory to another, it is difficult to make cross-laboratory comparisons of results reported in literature. To avoid delving into this complexity, we aimed to highlight qualitative and quantitative structure-activity relationships (QSAR) which govern the activity and stability of metallomacrocyclic complexes, which when well understood, refined and carefully implemented should constitute a fundamental gateway for rational design of better catalysts.

Metalloporphyrins and metallophthalocyanines show very similar physico-chemical properties and are structurally related to biological catalysts like cytochrome c and haemoglobin. The basic difference between their structures is shown (Fig. 1). As it will be shown in details later, the properties of these complexes are very dependent on the type of central metal (M), and on the nature of the substituents on the ligand.

Figure 2 presents the research growth rate of the use of metalloporphyrins and metallophthalocyanines as electrocatalyst for ORR in the last three decades (1982–2011). The

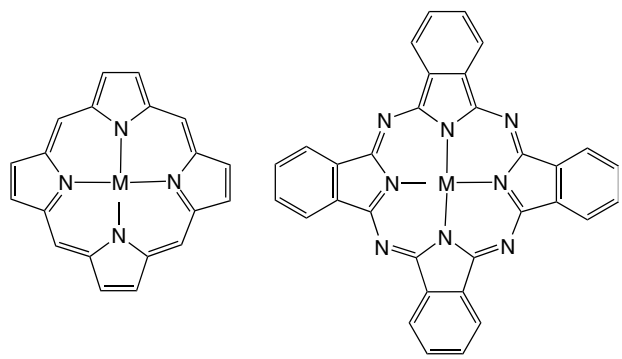

Fig. 1. Basic structure of a metalloporphyrin (a), and a metallophthalocyanine (b)

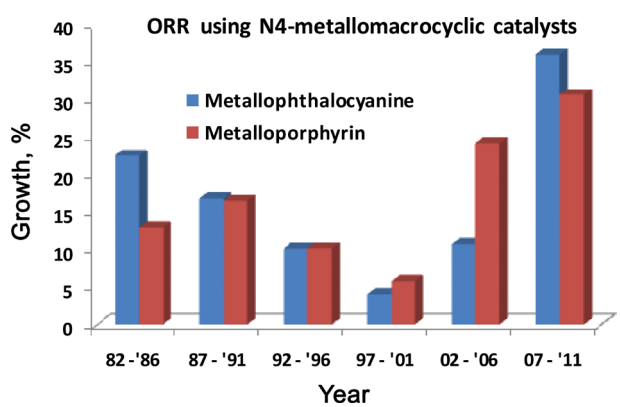

Fig. 2. Graphical representation of the publication growth (% growth = number of publications per 5-year period divided by the total number of publications in the last 30 years, multiplied by 100) from 1982 until 2011. Raw data obtained from SciFinder Scholar(R) search engine

Table 1. Possible pathways for oxygen reduction in aqueous media

Mode of interaction	ORR pathways	
	Acidic medium	Basic medium
	$O_2 + 2e^- + 2H^+ \rightarrow 2OH_{ads}$	$O_2 + 2e^- + 2H_2O \rightarrow 2OH_{ads} + 2OH^-$
	$2\ OH_{ads} + 2H^+ + 2\ e^- \rightarrow 2\ H_2O$	$2\ OH_{ads} + 2e^- \rightarrow 2OH^-$
Bridge	Overall direct reaction:	Overall direct reaction:
(or)	$O_2 + 4H^+ + 4e^- \rightarrow 2H_2O$;	$O_2 + 2H_2O + 4e^- \rightarrow 4OH^-$;
Trans	$E^o = 1.23$ V *vs.* NHE	$E^o = 0.401$ V *vs.* NHE
	$O_2 + e^- + H^+ \rightarrow HO_{2,ads}$	$O_2 + H_2O + e^- \rightarrow HO_{2,ads} + OH^-$
	$HO_{2ads} + e^- + H^+ \rightarrow H_2O$	$HO_{2ads} + e^- \rightarrow HO_2^-$
End-on	Overall indirect reaction:	Overall indirect reaction:
	$O_2 + 2e^- + 2H^+ \rightarrow H_2O_2$;	$O_2 + H_2O + 2e^- \rightarrow HO_2^- + OH^-$;
	$E^o = 0.682$ V *vs.* NHE	$E^o = -0.076$ V *vs.* NHE
	with $H_2O_2 + 2H^+ + 2e^- \rightarrow 2H_2O$;	with $HO_2^- + H_2O + 2e^- \rightarrow 3OH^-$;
	$E^o = 1.77$ V *vs.* NHE	$E^o = 0.88$ V *vs.* NHE

graph is interesting as it clearly depicts that the research interest in ORR by metallomacrocyclic complexes follows the trends in global oil prices and world events; increasing as the oil prices increase, and reduces as the oil prices reduce (see "Oil price history and analysis" at: http://www.wtrg.com/prices.htm). The period 1981/82 recorded one of the peak oil prices in the world. The increased research in the 1982–1986 period may be related to two major events that led to high oil prices; the Iran/Iraq war and the imposition of price controls by the US on her domestically produced oil, resulting in the US consumers paying more for imports than domestic production. The increased research activity in the 1987–1991 period is associated with the spike in oil prices in 1990 due to low production and uncertainty related to the Iraqi invasion of Kuwait and the ensuing Gulf war. Crude oil prices were low in the 1992–1996 period (about US$ 20 per barrel). The 1997–2001 period was the period of the Asian financial crisis that led OPEC to increase oil production quota by 10%. In fact, this period recorded one of the lowest oil prices in history (about US$ 18 per barrel in 1998). It is not surprising that the research activities in ORR for fuel cells and metal-air batteries were at their lowest at this period. Since 2002 to date, research on ORR has continued to increase due to high oil prices as a result of the Asian economic growth, weak US dollar, Iraq war, world economic recession, and the Arab uprising termed the "Arab spring."

Reaction pathways for the reduction of molecular oxygen

The electrochemical reduction of oxygen in aqueous solutions is a complex multi-electron reaction that occurs *via* two main pathways: one involving the transfer of two electron to give peroxide, and the so-called direct 4-electron pathway to give water. The latter involves the rupture of the O–O bond. The nature of the electrode strongly influences the preferred pathway. Most electrode materials catalyse the reaction *via* two electrons to give peroxide. The several possible pathways are summarized in Table 1.

In strongly alkaline solutions or in organic solvents, O_2 is reduced via the transfer of a single electron to give superoxide ion

$$O_2 + e^- \leftrightarrows O_2^- \quad E^\circ = -0.33 \text{ V} \quad \textit{vs.} \text{ NHE}$$

The maximum free energy or the highest oxidant capacity of O_2 is obtained when this molecule reacts on the cathode of a fuel-cell *via* 4-electrons. So there is a need for catalysts that promote the 4-electron reduction pathway. Most common electrode materials only promote the 2-electron pathway, which releases almost one half the free energy compared to that of the 4-electron pathway. This is due in part to the relatively high dissociation energy of the O–O bond (118 kcal/mol). The 4-electron reduction of dioxygen to give water involves the rupture of the O–O bond and can involve the interaction of dioxygen with one site (single site) or with two active sites simultaneously (dual site) on the electrode surface (Fig. 3).

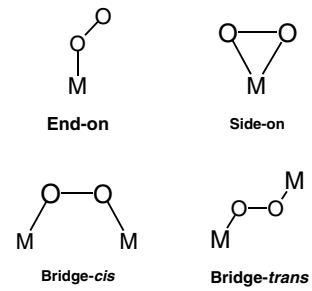

Fig. 3. Different special configurations for molecular oxygen when it interacts with metal sites

Upon these possible interactions, the energy of the O–O bond decreases, favoring its rupture since electrons accepted by the oxygen molecule will occupy antibonding π* orbitals. On platinum, O_2 reduction occurs almost entirely *via* 4-electrons [17]. It is likely that on this metal O_2 interacts *via* "bridge cis" conformation, involving two metal active sites (see Fig. 3) since the Pt–Pt separation in certain crystallographic orientations is optimal for this type of interaction. It is then crucial to develop low cost catalysts that decrease the overpotential of the reduction of oxygen and that can also promote the 4-electron reduction pathway.

Determination of the selectivity of oxygen electroreduction

Ordinarily, the selectivity of ORR is determined by means of rotating disk electrode (RDE) or rotating ring-disk electrode (RRDE) voltammetry. The RDE is designed to boost the diffusion of an electroanalyte in conditions where an electrochemical reaction is limited by diffusion of the analyte to the electrode. In RRDE, a ring (often platinum) surrounds the disk electrode with an insulating material (usually Teflon) between them (Fig. 4). During rotation of the electrode, the electrolyte is tangentially drawn to the disk electrode and radially swept away from it under controlled hydrodynamic conditions. Levich showed that the diffusion limited current (i_d) measured at a smooth disk electrode under controlled rotation is related to the angular velocity speed of rotation of the electrode according to Equation (1) [18];

$$i_d = 0.62nFAD_0^{2/3}\omega^{1/2}\upsilon^{-1/6}C_0 \quad (1)$$

where n is the number of electrons exchanged per molecule, F is the Faraday constant, A is the surface area of the electrode, D_0 is the diffusion coefficient of the electroanalyte, ω is the angular velocity of the electrode, υ is the kinematic viscosity of the electrolyte and C_0 is the bulk concentration of the electroanalyte. For a reaction which is essentially under diffusion limitation, a graph of i_d against $\omega^{1/2}$ yields a straight with a slope $= 0.62nFAD_o^{2/3}C_o\upsilon^{-1/6}$ from which n may be determined. Note that the coefficient 0.62 is used when ω is expressed in rad s^{-1}, while 0.21 is used when ω is expressed in revolution per minute (*i.e.* $0.62 \times (2\varpi/60)^{1/2} = 0.21$) [19]. A more commonly used approach employs a modified form of Equation (1), called the Levich–Koutecky analysis Equation (2), for reactions which are under mixed kinetic and diffusion control; where i is the measured current, i_k is the kinetic current defined by Equation (3) and i_d is the term in Equation (1).

$$\frac{1}{i} = \frac{1}{i_k} + \frac{1}{B\sqrt{\omega}} \quad (2)$$

$$i_k = knAFC_0 \quad (3)$$

From Equation (2), a graph of the inverse of the measured current at a given potential i^{-1} against $\omega^{-1/2}$ gives a straight line with a slope of B^{-1} from which n can be determined, and i_k^{-1} as the intercept on the i^{-1} axis [18].

The RRDE is designed in such a way that under the hydrodynamic conditions, an electroactive species generated at the disk may be detected at the ring electrode. The species generated at the disk electrode must therefore be sufficiently long-lived to be able to traverse the radius of the disk electrode and be detected at the ring. For the case of the ORR, the ring electrode is always poised at a potential where any H_2O_2 generated at the disk is oxidized at the ring. The fraction of H_2O_2 generated during ORR is calculated from Equation (4);

$$X_{H_2O_2} = \frac{2I_R / N}{I_D + I_R / N} \quad (4)$$

where N is the collection efficiency of the ring electrode, I_R is the ring current and I_D is the disk current. The value of N is normally supplied by the manufacturer but it advisable to verify it as often possible using a suitable redox pair [20].

The RDE and RRDE are very convenient techniques for studying the mechanism and kinetics of ORR and are by far the most widely used methods. However, it is important to bear in mind that the underlying mathematical formulations of these methods are theorized for smooth electrode surfaces under lamninar flow hydrodynamics. There are many examples in recent literature where RDE and RRDE have been used to study catalyst films for which turbulent flow hydrodynamics is quite obvious. The collection efficieny of RRDE for microscopically disordered films, for example

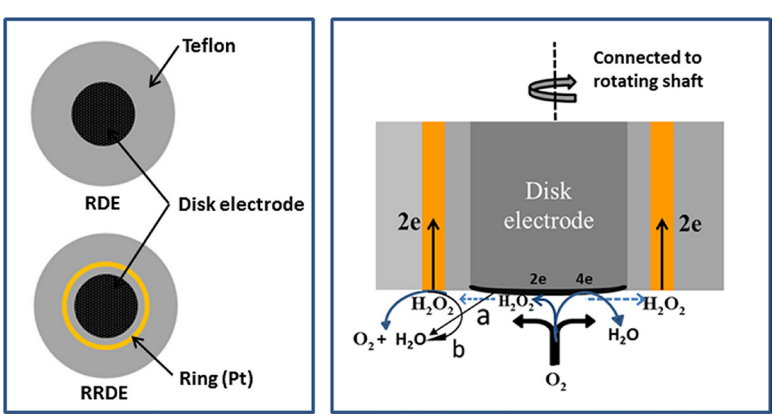

Fig. 4. Schematic representation of the RDE and RRDE (left panel), and of the possible reactions that takes at the RRDE during ORR (right panel)

very porous materials and irregularly built-up films (as may be the case for catalysts modified with nanocarbons such as carbon nanotubes and graphenes), is likely to be determined erroneously due to sporadic hydrodyamics. Therefore, the quality of a given catalyst film has a great influence on the correctness of results obtained from RDE and RRDE. It is generally recommended that catalyst films for RDE and RRDE studies should be as thin as possible [20]. Thick films may lead to increased mass-transport resistance through the catalyst layer and incomplete utilization of the catalyst which certainly lead to incorrect interpretation of results. These factors have to be considered critically when performing and interpretating RDE and RRDE measurements. A depiction of the possible processes that occur during the electroduction of oxygen at RRDE electrodes is schematically shown in Fig. 4 to draw attention to some possible sources of error in treatment and interpretation of RRDE results. If O_2 is reduced by the transfer of two electrons to form H_2O_2, at least four competing reactions may follow and these include: a competition between further electroreduction of H_2O_2 and its disproportionation on the disk, and if the H_2O_2 makes it to the ring, a competition between its electrochemical detection and disporportionation takes place since H_2O_2 is known to disporportionate on Pt surfaces. Therefore, the amount H_2O_2 detected at the ring is likely to be much lower than the amount actually produced because of the competing reactions. The magnitude of the error encountered in the determination of n and H_2O_2 using RRDE is likely to be even larger the less smooth the catalyst film is. However, in the absence of a more reliable method for studying the mechanism and kinetics of ORR, RDE and RRDE voltammetry continue to be useful and handy. In the face of these drawbacks, several groups have proposed the use of scanning electrochemical microscopy (SECM) to study the selectivity of electrocatalysis of ORR [21].

FROM MODEL STRUCTURES TO ACTIVE N_4-METALLOMACROCYCLIC CATALYSTS

The ORR pathway by N_4-metallomacrocyclic complexes is dependent on very many factors, as such; the ambiguity surrounding the pathways of ORR by these complexes is as enormous as the number of publications about the subject. In this section, a discussion of ORR by N_4-metallomacroyclic complexes is given with special emphasis placed upon those complexes and their design aspects which facilitate the four-electron reduction of oxygen. Nature achieves facile reduction of oxygen to water in the terminal respiration chain by cytochrome c oxidases (CcO) at their heme (Fe a_3)/Cu (Cu_B) bimetallic active site (Fig. 5a) at very high turn-over frequencies. This makes CcO interesting model systems to emulate, in what should be appropriately termed as bioinspired catalyst design. The next section gives a brief insight of the electrocatalysis of oxygen reduction by CcO and the progress attained in the biomimetic design of artificial heme/Cu like catalysts for oxygen reduction.

Oxygen reduction by cytochrome c oxidases

Natural cytochrome c oxidases (CcO) catalyze the reduction of oxygen at their heme a_3/Cu_B (Fig. 5a) bimetallic site directly to water without the release of superoxide or peroxide. The Fe–Cu distance in CcO varies in the range of ~4.9–5.3 Å [22] depending on the redox states of the metal ions and ligation thereof, influenced by the protein environment. Collman *et al.*, have recently provided additional evidence that the active site in CcO is comprised of a heme a_3 of an iron porphyrin and Cu (Cu_B) coordinating three histidine groups with one of the histidine groups bound to a post-translationally modified

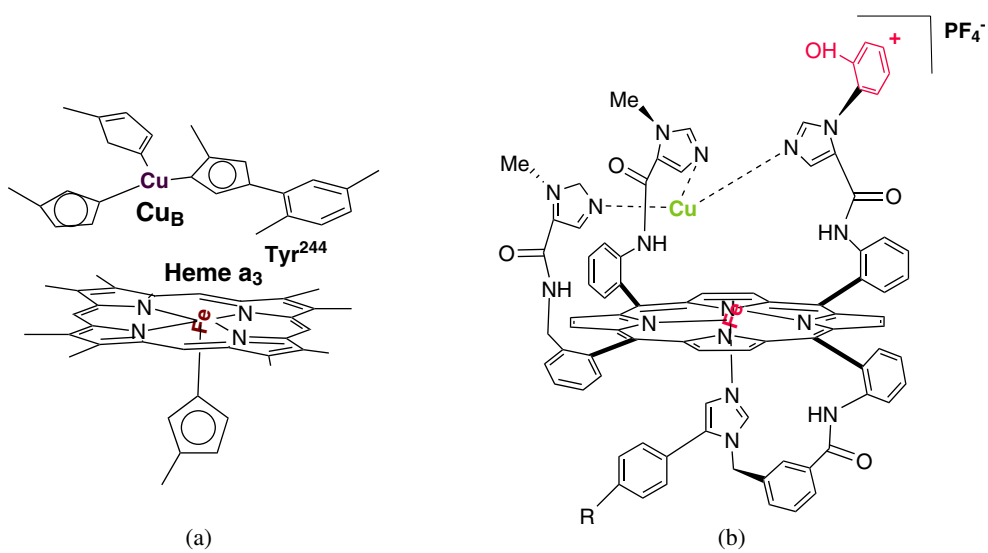

Fig. 5. Active structure of cytochrome c oxidase (a), and of a synthetic analogue of cytochrome c oxidase (b). Reprinted with permission from [23] *American Chemical Society*

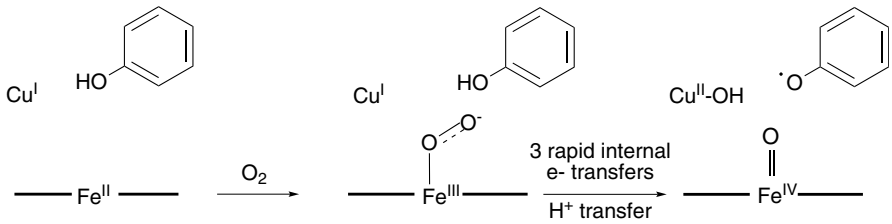

Fig. 6. A simplified mechanism leading to formation of the oxidized intermediate in the course of oxygen reduction at the active site of a functional heme/Cu analog of CcO. Reprinted with permission from [23] *American Chemical Society*

tyrosine residue (Fig. 5b) [23]. It is reported that the primary role of the redox centres is to rapidly provide the four-electrons needed to reduce oxygen directly to water without the release of toxic superoxide or peroxide species.

The mechanism of reduction involves adsorption of oxygen at the reduced Fe^{II}/Cu^{I} centre to form an Fe^{III}-O_2^- superoxide adduct with subsequent formation of an intermediate comprised of oxidized Cu^{II}, an Fe^{IV}=O ferryl radical, and a peripheral phenoxide radical (Fig. 6). The oxidized intermediate is then reduced directly to water by simultaneous transfer of four-electrons [23].

Tremendous effort has been devoted to synthesize artificial catalysts which can achieve reduction of oxygen directly to water by mimicking the active site of CcO [23]. A key motivation of this endeavour has also been to use the CcO synthetic analogs as biomimetic models to probe the structure and function of CcO in the respiration chain. After an enduring effort spanning about three decades, successful synthesis of a functional heme/Cu analog with the ability to reduce oxygen directly to water at physiological conditions without generation of toxic peroxide and superoxide species was reported [22–25]. It is generally believed that natural enzymes exhibit unique flexibility, with the ability to sustain long range open-to-closed conformational changes, which is necessary for binding and catalysing the reaction of small molecules [26]. Synthetic mimics of the heme/Cu active site in CcO must therefore be faultlessly designed with such conformational flexibility as to facilitate adsorption of oxygen, retention of partially reduced oxide species (PROS) intermediates until final products are formed, and release of the products. Artificial analogs of the heme/Cu sites in CcO have tended to be rather rigid, devoid of this conformational flexibility. A number of factors which complicate replication of the heme/Cu site of the CcO system in biomimetic design of functional heme/Cu analogs for oxygen reduction have been discussed [25]. Functional analogs of CcO incorporating dissimilar metal centers other than a heme/Cu active site have also been reported [27]. The success achieved in synthesizing functional CcO analogs and in the elucidation of their mechanism for oxygen reduction is not only useful for understanding the role of CcO in the terminal respiration chain, but also gives new impetus to the design of effective molecular catalysts for four-electron reduction of oxygen.

Oxygen reduction by bimetallic cofacial porphyrins

Dicobalt cofacial diporphyrins hinged on amide bridges were the earliest bimetallic diporphyrins with close semblance to the heme/Cu system that achieved four-electron reduction of oxygen to water in acidic electrolytes at remarkably low overpotentials [28]. Minor alterations in the dicobalt diporphyrin structures are reported to drastically poison the potency of the catalysts, or causes them to revert to two electron oxygen reduction catalyts [29]. Selection of the right anchoring system for the two individual cobalt porphyrin units to achieve just the right interplanar conformational separation between them is one critical factor in designing dicobalt cofacial diporphyrins with the ability to reduce oxygen to water. The first successful bridging system for two dicobalt diporphyrins was reported by Collman *et al.* and comprised of two diametrically positioned four-atom amide chains [28, 30]. The potential at which oxygen reduction commences in these complexes is substantially more positive than the standard potential of the O_2/H_2O_2 couple (E = 0.68 V *vs.* SHE) which thermodynamically precludes production of hydrogen peroxide by any mechanism.

When one or both cobalt atoms were replaced by other metal atoms, hydrogen peroxide was formed either as the main product or as an intermediate. Chang *et al.* found that dicobalt diporphyrins anchored on dibenzofuran (DBD) and xanthene (DPX) Fig. 7A, exhibited remarkable conformational flexibility, and in both cases, the complexes were able to reduce oxygen directly to water despite large differences (~4 Å) in the interplanar

Table 2. Dicobalt cofacial porphyrins with a high selectivity for direct four-electron reduction of oxygen

Electrocatalyst	Medium	$E_{1/2}$(V) *vs.* NHE	n	Reference
Co_2FTF4	0.5 TFA	0.71	3.9	[28]
Co_2DPB	0.5 TFA	0.70	3.7	[31]
Co_2DPA		0.67	3.7	[31]
Co_2DPD	0.5 M $HClO_4$	*ca.* 0.57	4	[26]
Co_2DPX	0.5 M $HClO_4$	*ca.* 0.58	4	[26]
$[Ir(OEP)]_2$DDAB	0.5 M H_2SO_4	0.80	4	[40]
$[Ir(OEP)]_2$	0.1 TFA	0.57	4	[39]

DDAB = Didodecyldimethylammonium bromide; TFA = trifluoroacetic acid

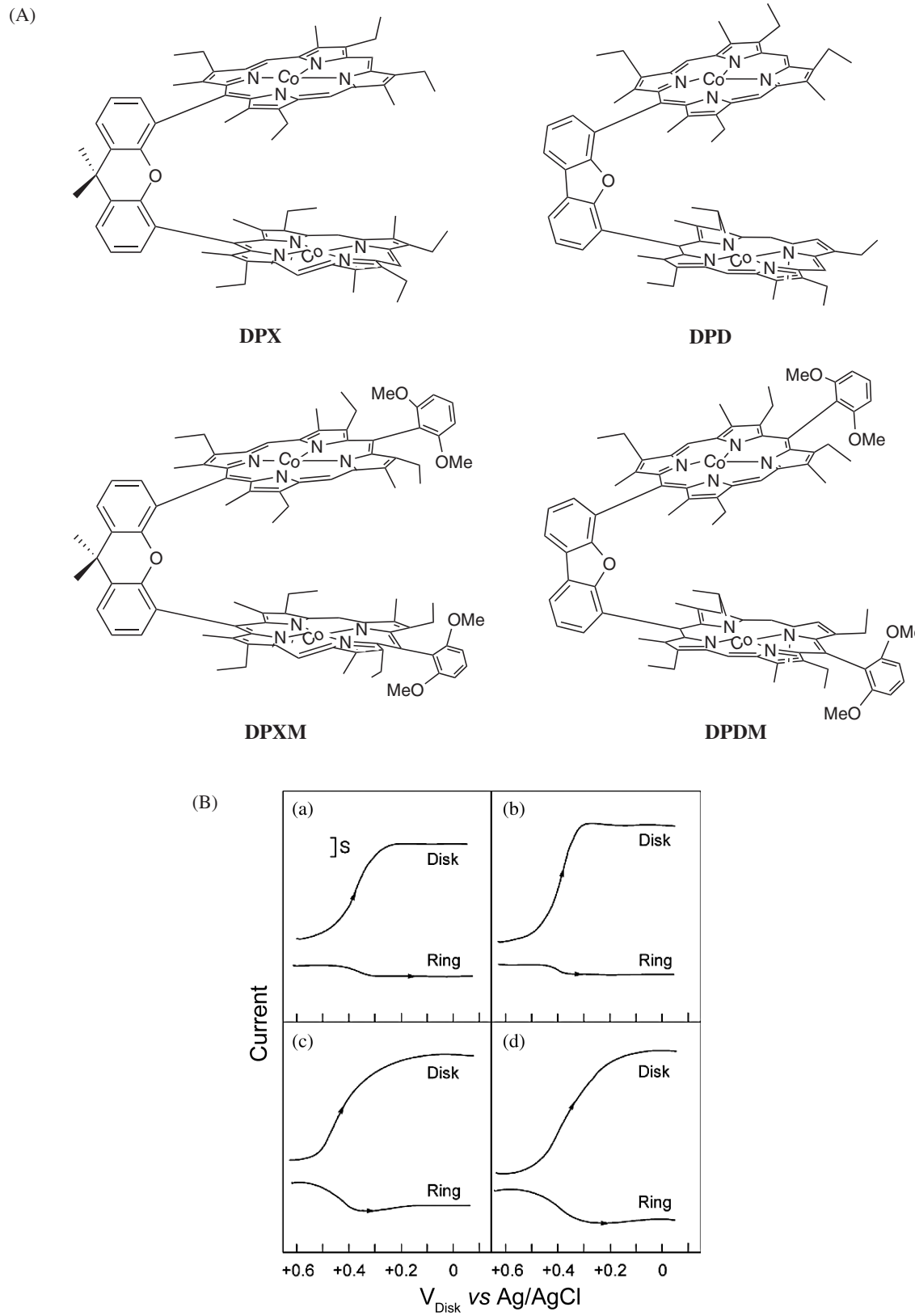

Fig. 7. (A) Examples of dicobalt cofacial bisporphyrins: DPX = diporphyrin xanthene (a); DPD = diporphyrin dibenzofuran (b); DPXM = diporphyrin xanthene methoxyaryl (c); diporphyrin dibenzofuran methoxyaryl (d). (B) Rotating ring-disk voltammograms of O_2 reduction at pyrolytic graphite disks modified with (a), (b) (c) and (d). Reprinted with permission from [37] *American Chemical Society*

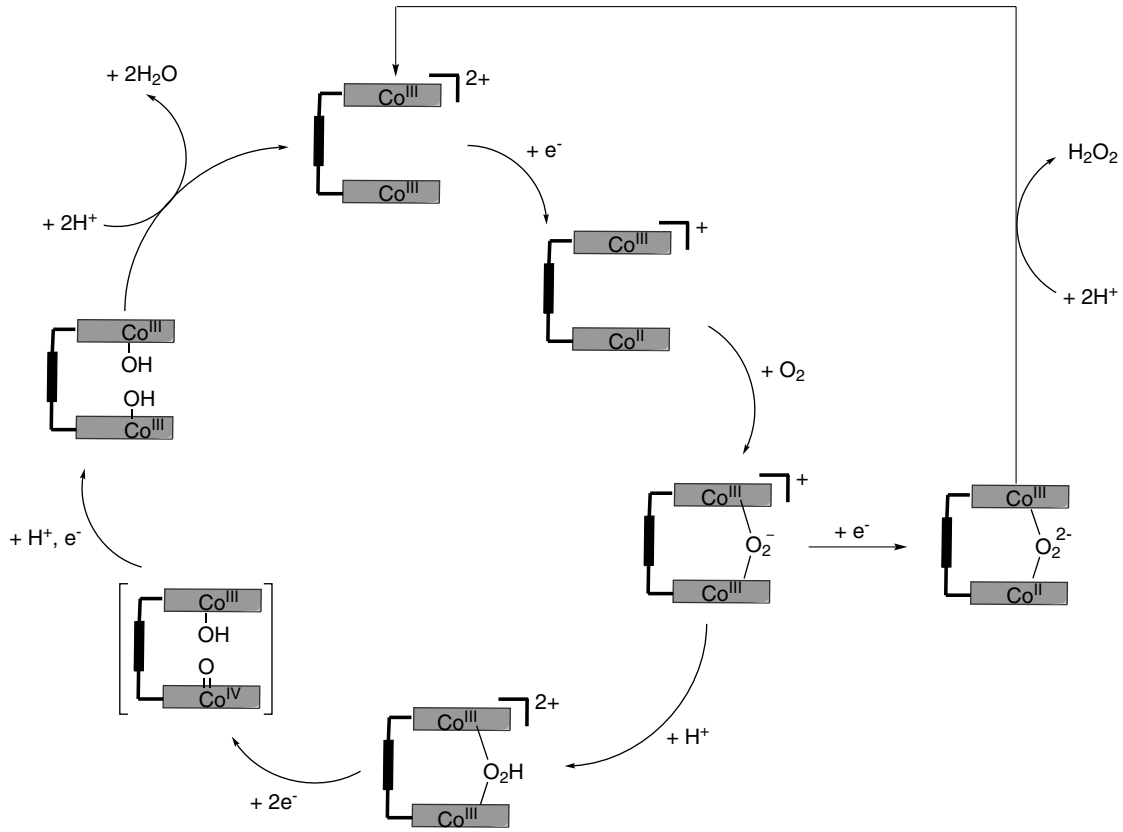

Fig. 8. Proposed mechanism for oxygen reduction at an active site of a dicobalt cofacial diporphyrin. Adopted from reference. Reprinted with permission from [37] *American Chemical Society*

separation of their metal centers [26]. Two other anchoring systems, anthracene and bisphenylene have also been successfully used to design four-electron oxygen reduction "Pillared" cobalt(II) cofacial diporphyrins (Fig. 7A) [31, 32]. The flexibility of the dicobalt cofacial porhyrins anchored on DPD and DPX was attributed to the ability of these hinge-like frameworks (or Pillard platforms) to considerably open their bite "the Pac-Man effect" in accommodating exogenous ligands. The effect of the type of anchoring system and porphyrin structure on the ORR activity of dicobalt cofacial diporphyrins can be observed in Fig. 7B. The ORR activity is drastically affected by the introduction of 2,6-dimethoxyphenyl groups to the *meso*-position of the porphyrin ring as can be seen by the increased anodic current registered at the ring. It is however not definitively clear whether it is the electronic changes or steric effects which lead to this sharp drop in activity. Some quantitative results showing the effect of the type of anchoring system on the ORR activity of dicobalt cofacial porphyins were reported in the review by Collman *et al.* [33].

The two cobalt centers in dicobalt cofacial diporphyrins have been reported to act in concert in order to achieve four-electron reduction of oxygen [34, 35]. One of the sites reportedly functions as a Lewis acid to stabilize the intermediate(s) in the cavity, ensuring that it does not dissociate before completion of the reaction [36]. To corroborate the dual site postulate and specificity of the reaction site, a parallel type of mechanism involving both the two and four-electron reduction was observed when one of the Co(III) centers in Co_2FTF4 was replaced with Al(III). A simplified scheme of the proposed mechanism of oxygen by dicobalt cofacial porphyrins is shown in Fig. 8 [37].

A rather unusual drawback associated with dicobalt cofacial diporphyrins is their drastic decline in activity when adsorbed on other electrode surfaces other than edge plane graphite (EPG). The catalysts have been reported revert to two electron reduction catalysts when adsorbed on other electrode surfaces other than EPG [33]. This has led to the conclusion that axial ligation of surface oxygen groups on EPG to the cobalt ion bears a significant contribution to the ORR activity of these complexes [33]. A second disadvantage is that these complexes are active in limited potential and pH windows outside of which they become readily deactivated. In a particular study which investigated the influence of site availability of these complexes for oxygen adsorption, and for axial ligation on their activity for oxygen reduction, that is, whether the sites were located inside or on the outside of the cavity, found that four-electron reduction of oxygen was only possible when the sites inside the cavity were both available for interaction with oxygen. As with monomeric monuclear porphyrins, dicobalt cofacial diporphyrins

also gradually lose their activity upon repetitive potential cycling for a few cycles. Pretreatment of the active catalysts with hydrogen peroxide was found to rapidly deactivate them thus indicating that the mechanism of their deactivation involved chemical attack of the adsorbed dicobalt cofacial diporphyrin by peroxide and superoxide species. Despite all these existing drawbacks, the success achieved thus far should stimulate enthusiasm for synthesis of molecular heme/Cu or heme/Cu-like analogs of CcO, and dinuclear cofacial porphyrin which can function under the conditions desirable for technological applications. As proposed way back in the original work by Collman *et al.*, it should be possible to modulate the ORR activity of the dicobalt cofacial porphyrins by judicious modification of the porphyrin ring, and possibly by exploration of other bridging groups [28].

Oxygen reduction by simple N_4-metallomacrocyclic complexes

The enormous amount of literature available about the pathways for oxygen reduction by simple N_4-metallomacrocyclic complexes, which conflicts in some cases, complicates a balanced review of the work. Additionally, the activity and stability of N_4-metallomacrocyclic complexes are affected by a variety of factors as spelt out in the introduction. This makes it difficult to make reliable cross-laboratory comparisons. However, by and large, the number of simple N_4-metallomacrocyclic complexes that can achieve the reduction of oxygen exclusively to water without generation of substantial amounts of hydrogen peroxide is generally very limited. Much of the attention in this section is devoted to research frontiers in view of promising simple N_4-macrocyclic catalysts that can achieve four-electron reduction of oxygen as this is the primary desire of many researchers in the field. To simplify our task, bearing in mind that thorough coverage of all the important works reported over the last four decades by various authors cannot be achieved faultlessly, emphasis of the discussion was placed more on specific structural properties, or special catalyst preparation procedures that achieve four-electron reduction of oxygen either: (i) in a direct four reduction process or (ii) in a series process *via* hydrogen peroxide as an intermediate with its further electrochemical reduction to water or dismutation to water and oxygen, or (iii) in a parallel type mechanism involving both (i) and (ii). Unique cases involving sophisticated modifications, or otherwise, by means of which oxygen is reduced by the transfer of four electrons have also been included in as far as we could access the concerned literature. The rationale for discussing the electrocatalysis of oxygen reduction by these complexes in slight detail was to draw attention to their important properties which furnish them with the unique ability to facilitate the four-electron reduction of oxygen.

Direct four-electron reduction of O_2 by simple monomeric N4-macrocycles. Most simple monomeric, monometallic N_4-metallomacrocyclic complexes can only achieve the reduction of oxygen to hydrogen peroxide by the transfer of two electrons. Some of these complexes can however catalyse the reduction of oxygen in a direct four-electron transfer process and they constitute the subject of discussion in this section.

A number of iridium porphyrins; Ir(OEP)R, R = H, alkyl or aryl derivatives, and Ir(OEP)I and Ir(OEP)OOH catalyze the direct four-electron reduction of oxygen at substantially low overpotentials [38]. With the exception of Ir(OEP)H, the rest of the complexes required preconditioning at specific potentials to be activated, the required conditioning potential varying depending on the nature of substituent groups. Specifically, Ir(OEP)R complexes required conditioning at high positive potentials (>0.8 V *vs.* NHE), while Ir(OEP)I and Ir(OEP)OOH required conditioning at negative potentials (< -0.2 V *vs.* NHE) to be activated [39]. As can be seen in Fig. 9a, Ir(OEP)H has been reported to exhibit the best activity similar to, or better than that observed for dicobalt cofacial porphyrins [38, 39]. It was reported in a particular study that the presence of a cationic surfactant (DDAB) improved both the activity and stability of Ir(OEP)H and also widened its active potential window, Fig. 9b [40].

The dimeric form of Ir(OEP), $[Ir(OEP)]_2$ also catalyses the direct four-electron reduction of oxygen but unlike its monomer, it does not require any conditioning. As shown in Fig. 9a, the iridium chelate complexes become severely but reversibly deactivated at low potentials [41]. Their activity is not however affected by pH as dramatically as the dicobalt cofacial diporphyrin complexes. As with the case for Co_2FTF catalysts, it was reported that when the Ir(OEP)R catalysts are adsorbed on other electrode surfaces other than EPG, their activity declines to two electron reduction catalysts. Quite surprisingly, the main product of oxygen reduction was reported to be hydrogen peroxide after pyrolysis of Vulcan supported IrOEP and IrTPP. This is a rather peculiar case since most N_4-metalloporphyrins increase in activity upon pyrolysis. It has also been reported that the Ir complexes are unstable in air, losing all their activity after a few months. The four-electron reduction of oxygen by iridium porphyrins was attributed to a single site which facilitates side-on adsorption of oxygen on Ir(II), and that scission of the O–O bond was a likely step in the mechanism. Unfortunately, Ir is one of the rarest and most expensive metals which would render its use very costly. Nonetheless, the complex should serve as a suitable model, such that theoretical and experimental knowledge gained from its study, may serve to tailor the synthesis of improved catalysts.

The other monomeric mononuclear porphyrins which mediate the four-electron reduction of oxygen are cobalt porphine (CoP) and cobalt *meso*-tetramethyl porphyrin (CoTMeP) with CoP exhibiting higher activity than CoTMeP [42]. The unexpectedly high activity of CoP was attributed to its likely spontaneous

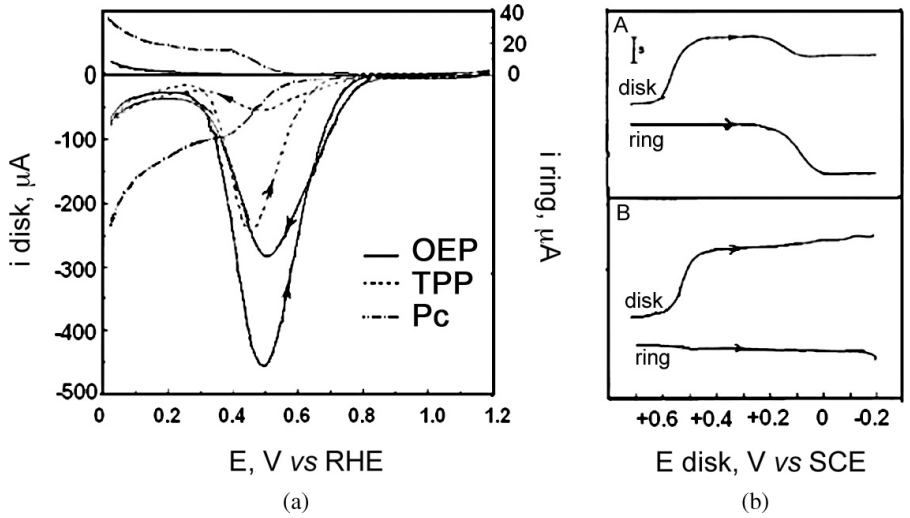

Fig. 9. (a) Rotating ring-disk voltammograms of iridium-chelates irreversibly adsorbed on pyrolytic graphite in 0.5 M H_2SO_4 at a rotation of 16 rps and scan rate of 10 $mV.s^{-1}$. Reprinted with permission from [41] Elsevier, (b) rotating ring-disk voltammograms of a Pt (ring) and graphite (disk) coated with DDAB and $[Ir(OEP)]_2$ (1.3×10^{-9} mol cm^{-2}) upper panel (A), and lower panel (B) Pt ring (uncoated)-Pt disk in 0.5 M H_2SO_4 saturated with air. The Pt rings were maintained at 1.0 V in both cases. Reprinted with permission from [40] *Elsevier*

dimerization to produce a more catalytically active species. The synthesis of CoP or its free base (porphine) still presents a challenge with regard to attainable yields and purity, which makes it overly expensive for a non-precious metal catalyst. It is also regrettable that the catalyst is highly susceptible to oxidative degradation which severely affects its attractiveness. In a later study which compared the ORR activity of several *meso*-tetraalkyl cobalt porphyrins by the same group, activity was found to follow the order: CoP > CoTmeP > CoTBuP > CoTPrP > CoTEtP > CoPeP [13]. This led to the conclusion that the rate of adsorption of oxygen decreased as the bulkiness of the alkyl substituents increased. At the moment, there is no foreseeable strategy for improving the stability of CoP. Nevertheless, understanding the properties of CoP which furnish it with this exceptional activity should serve to guide the synthesis of better catalysts.

Table 3. Metalloporphyrins with high activity and significantly low overpotentials for oxygen reduction in acidic electrolytes

Electrocatalyst	Medium	$E_{1/2}$(V) *vs.* NHE	(n)	Reference
Ir(OEP)H	0.1 M TFA	0.72/0.8	3.9	[38]
IrTPP	0.1 M TFA	0.48	NR	[39, 41]
Ir(OEP)R, R = OOH, Ph	0.1 M TFA	0.54	NR	[39]
CoP	1 M $HClO_4$	0.75	3.8	[42]
CoTMeP	1 M $HClO_4$	0.64	3.3	
$[CoP(pyRu(NH_3)_5)_4]$	0.5 M $HClO_4$	0.47	NR	[35]
$[CoP(PhCNRu(NH_3)_5)_4]$	0.5 M $HClO_4$	0.58	NR	[35]
$[CoP(py\text{-}CH_3)_4(Os(NH_3)_5)_{-2}]$	0.5 M $HClO_4$	0.59	NR	[35]

NR = not reported; n = number of electrons transferred

Four-electron O_2 reduction by specially modified N_4-metallomacrocyclic complexes

Certain modification procedures have been shown to yield N_4-macrocyclic complexes which afford the reduction of oxygen in a four-electron process. For example, it was reported that cobalt (tetrakis(4-pyridyl)porphyrin), with four $[Ru(NH_3)_5]^{2+}$ or ($[(NH_3)_5Os]^{n+}$ (n) 2, 3) groups around the porphyrin periphery, generally termed as "multinuclear catalysts" reduce oxygen nearly exclusively to water [35, 43, 44]. The evident increase in the diffusion limited current for oxygen reduction at the disk and the large decrease in the anodic current at the platinum ring (Fig. 10b) clearly confirm that modification of $CoP(py)_4$ with $[Ru(NH_3)_5]^{2+}$ converts it from a predominantly two electron O_2 reduction catalyst to a nearly exclusively four-electron reduction catalyst with minimal generation of hydrogen peroxide.

The proposed mechanism for oxygen reduction by the multinuclear ORR catalysts is outlined in Fig. 11 for tetraruthenated $[CoP(pyRu(NH_3)_5)_4]^{8+}$ but is also applicable to osmiumated porphyrins.

The mechanism has been proposed to involve π-back donation from Ru(II) or Os(II) to the oxygen adsorbed porphyrin adduct Co(II)–O_2, where the cobalt porphyrin is the site for oxygen reduction while Ru and Os serve as co-catalysts which affect the relative rates of two competing pathways for the reduction of oxygen. The first step in the mechanism involves generation of Co(II) porphyrin with subsequent adsorption of oxygen on the Co(II) active site in the next reaction (2). The next reaction (3),

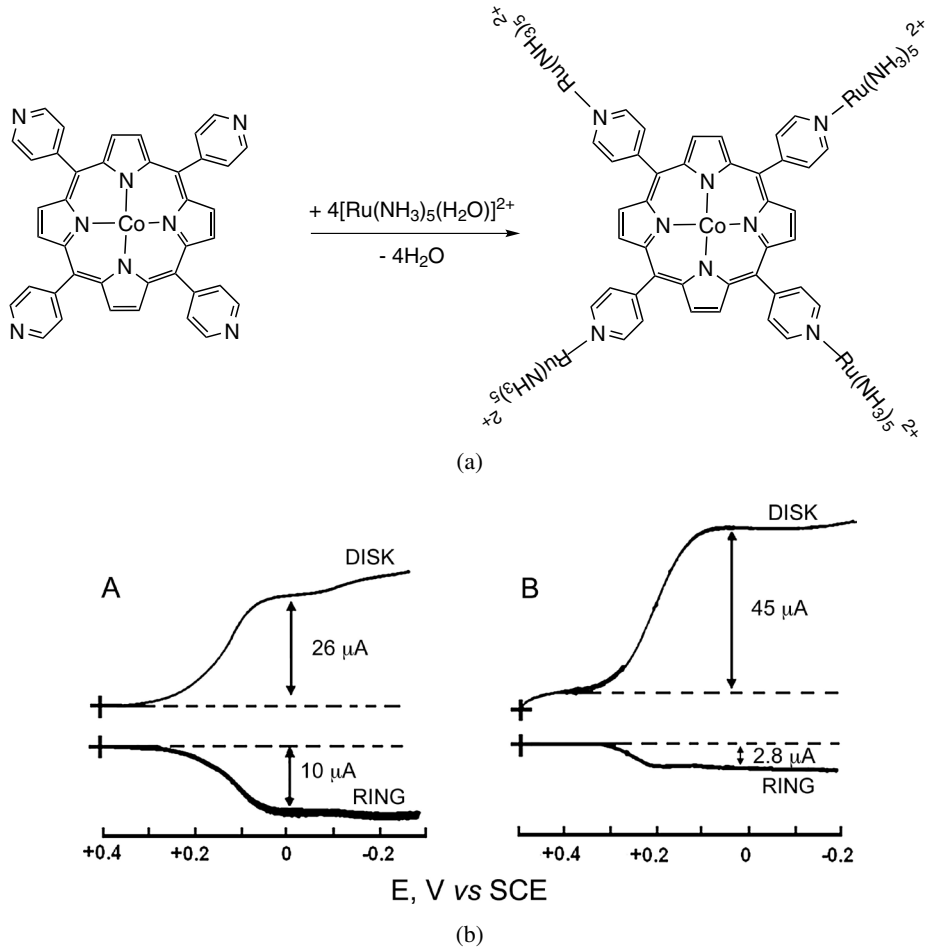

Fig. 10. (a) Reaction for conversion of $CoP(py)_4$ to $[Co^{II}P(pyRu^{II}(NH_3)5)^4]^{8+}$, adopted from Ref. 35 (b) RRDE voltammograms of (A) $CoP(py)_4$; (B) $[Co^{II}P(pyRu^{II}(NH_3)_5)_4]^{8+}$. Reprinted with permission from [43] *American Chemical Society*

$$\left[Co^{III}P(pyRu^{III}(NH_3)_5)_4\right]^{13+} + e^- \rightleftharpoons \left[Co^{II}P(pyRu^{III}(NH_3)_5)_4\right]^{12+} \quad (1)$$

$$\left[Co^{II}P(pyRu^{III}(NH_3)_5)_4\right]^{12+} + O_2 \rightleftharpoons \left[O_2CoP(pyRu^{III}(NH_3)_5)_4\right]^{12+} \quad (2)$$

$$\left[O_2CoP(pyRu^{III}(NH_3)_5)_4\right]^{12+} + 4e^- \rightleftharpoons \left[O_2CoP(pyRu^{II}(NH_3)_5)_4\right]^{8+} \quad (3)$$

$$\left[O_2CoP(pyRu^{II}(NH_3)_5)_4\right]^{8+} + 4e^- + 4H^+ \rightarrow \left[Co^{II}P(pyRu^{II}(NH_3)_5)_4\right]^{8+} + 2H_2O \quad (4)$$

$$\left[Co^{II}P(pyRu^{II}(NH_3)_5)_4\right]^{8+} + O_2 \rightleftharpoons \left[O_2CoP(pyRu^{II}(NH_3)_5)_4\right]^{8+} \quad (5)$$

Fig. 11. Proposed mechanism for O_2 reduction by $[CoP(pyRu(NH_3)_5)_4]^{8+}$ and other related multinuclear complexes. Reprinted with permission from [35] *American Chemical Society*

generates the back-bonding Ru(II) which drives the reduction of oxygen by four electrons as shown in reaction (4), and finally, regeneration of the Co(II)–O_2 in reaction (5). It has been proposed that the electronic effects produced by the back-donation of the Ru(II) and Os(II) complexes on Co(II)–O_2 might be achieved by other suitable electron-donating non-metallic functional groups attached to the porphyrin ring. It was however observed that differences in catalytic activity of multinuclear complexes were correlated to the relative back bonding strengths of the coordinated metal complexes but not on their relative reducing strengths. Monomeric Cobalt (tetrakis(4-pyridyl)porphyrin) with four $[Ru(NH_3)_5]_{2+}$ groups around the porphyrin periphery achieves reduction of oxygen to water when incorporated with nafion and adsorbed on EPG [45].

Ozoemena's group have recently reported that MOCPcPt (where M = Fe, Ru) (Fig. 12) supported on multi-walled carbon nanotubes affords the reduction of oxygen in a direct four-electron transfer process in 0.1 M NaOH [46, 47]. There was no significant difference between the ORR activity at the FeOCPcPt and RuOCPcPt except that the latter gave a slightly higher kinetic constant (~3.6 $\times 10^{-2}$ cms^{-1}) than the former (~2.8 $\times 10^{-2}$ cms^{-1}).

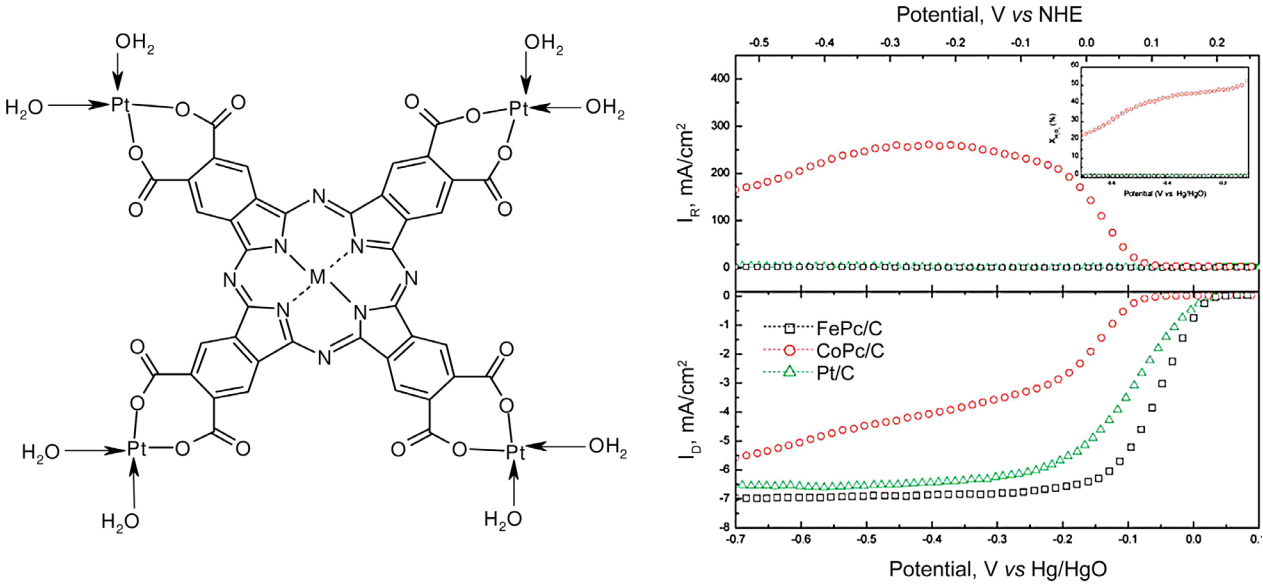

(a) (b)

Fig. 12. Structure of ruthenium tetrakis-(diaquaplatinum)octacarboxy phthalocyanine. Reprinted from [46] with the permission Wiley; (b) RRDE measurements of the ORR on the FePc/C, CoPc/C, and Pt/C electrodes at a rotation rate of 2500 rpm in a 0.1 M NaOH. Reprinted from Ref. [48] with the permission the *American Chemical Society*

Most cobalt porphyrins can only reduce oxygen to hydrogen peroxide with no further reduction or dismutation of the peroxide [49]. Some recent studies have proposed incorporating Prussian Blue (PB) or Horseradish peroxidase (HRP) into metalloporphyrin catalysts so that the hydrogen peroxide generated by the metalloporphyrin can be reduced further by the PB/HRP to water. For example, reduction of O_2 to H_2O was achieved by designing a multicomponent-multifunctional catalyst incorporating carbon nanotubes (CNTs), CoPIX, and PB. The CNTs provide a high surface area matrix for dispersion of the catalysts [50].

Electrodeposited iron tetrakis(*N*-methyl-4-pyridyl) porphyrin [51] and electropolymerized *meso*-tetrakis(2-thienyl)porphyrinato]cobalt(II) (pCoTTP) have been reported to reduce oxygen to water. The ability of pCoTTP to reduce O_2 directly to water was attributed to a conducting network of CoTTP nodal points where multiple layers are arranged in such a way that they form suitable Co–Co bifacial binding clefts for O_2, thus allowing four-electron reduction of oxygen to water. A study by Elbaz *et al.* has reported that Co(III) tetra(o-aminophenyl)porphyrin (Co(III)TAPP) and Co(III)(p-sulfonatedphenyl)porphyrin (Co(III)TPPS) incorporated into aerogel carbon (AEG) electrodes by adsorption or electropolymerization achieved four-electron of oxygen.

FUNDAMENTAL STUDIES OF O_2 ELECTRODUCTION BY N_4-METALLOMACROCYCLIC COMPLEXES

The disussion thus for focused mostly on qualitative description of the dependence of ORR activity on the structure of N_4-metallomacrocyclic complexes, and some special modification procedures which can be used to improve activity. In this section, much of the discussion will focus on quantitative description of the parameters which influence the ORR activity of N_4-metallomacrocyclic complexes. Specifically, the dependence of activity on the properties of the central metal ion will be dicussed in relation to the driving force of the reaction. In addition to this, the molecular orbital theory, and the concept of intermolecular hardness are used to describe the interaction between oxygen the central metal ion in N_4-macrocyclic complexes and how this interaction infleunces the ORR activity of the complex.

Effect of the central metal on the ORR activity of N_4-macrocylic complexes

The electroreduction catalyzed by N_4-macrocylic complexes is very sensitive to the nature of the metal center in the complex. For iron and manganese phthalocyanines, at low overpotentials a 4-electron reduction is observed with rupture of the O–O bond [12, 52, 53, 54], without the formation of peroxide. In contrast Co, Ni and Cu phthalocyanines promote the reduction of O_2 only *via* 2-electrons to give peroxide [12] as the main product of the reaction. Polymerized Co tetraamino phthalocyanines promote the 4-electron [55, 56] reduction whereas polymerized Fe tetraaminophthalocyanines only promote the 2-electron reduction [57] in contrast to their monomeric counterparts. The net catalytic activity of metal macrocyclics is linked to the redox potential of M(III)/(II) of the complexes, the more positive the redox potential, the higher the activity. This trend

is the opposite to what is expected from a simple redox catalysis mechanism, which is generally observed for the reduction of O_2 catalyzed by immobilized enzymes. The metal -N_4-chelates need to be supported on a conducting support, like carbon or graphitic materials. Long term stability is a problem with N_4-chelates. Heat treatment in an inert atmosphere increases both the stability and catalytic activity [58–61].

Even though a few studies have been carried out using the complexes in solution [62], most studies have been performed with the metal chelates confined on an electrode surface, generally graphite or carbon supports, since this is closer to the situation in a fuel cell, where catalysts are absent in the electrolyte. Since the support can act as an axial ligand, the properties of the complexes in solution or on the adsorbed state could be different. So most studies discussed here have been carried out with the complexes immobilized on graphite or carbon supports. Smooth electrodes have been used to study mechanistic aspects of the reaction.

Interaction of O_2 with active sites and the redox mechanism. The one-electron reduction of O_2 to give superoxide is an outer-sphere reaction and does not involve the interaction of the molecule with an active site on the electrode surface. The electron transfer process probably occurs at the outer Helmholz plane. This process is observed in non-aqueous media or in strongly alkaline aqueous solutions and is not relevant to fuel-cell development. In contrast, ORR occurring *via* the transfer of more than one electron (two or four) is an inner-sphere reaction, involving the interaction of the molecule and or intermediates with active sites present on the electrode surface. Since we are interested in discussing the electrocatalytic reduction of O_2, we will focus our attention on the inner-sphere reduction processes.

O_2 interacts with the N_4 catalysts usually binding to the d-orbitals of the central metal in the macrocyclic structure. The energy of the interaction will depend on the energy and the electronic density located on those orbitals. Figure 13 illustrates some different possible interactions (end-on and side-on) of the orbitals of the oxygen molecule with the orbitals of the metal in the M–N_4 molecule and Figure 14 illustrates the molecular orbitals diagram for end-on and side interaction respectively. For end-on M–O_2 complexes (see Figs 13 and 14), the most important interaction for both σ and π bonding occurs with the π* antibonding orbitals of the O_2. The σ interaction is primarily between the metal $3dz^2$ and the in plane antibonding π_g^s orbital on the O_2, where the superscript "s" refers to whether or not the orbital is symmetric (or antisymmetric) in relation to the MO_2 plane. This interaction involves a transfer electron density from the metal to the transfer to the O_2 molecule. The π interaction is primarily between the metal 3dyz and the $1\pi_g^a$ (π antibonding antisymmetric orbital) on the O_2 and can be viewed as a back-bonding interaction. In both of these interactions the π_u^s and π_u^a (bonding π orbitals symmetric and antisymmetric respectively) play a lesser role in the composition of the bonding orbitals [63]. In the case of the side-on interaction a $3dz^2$ orbital of the metal interacts with the $1\pi_s^u$ bonding orbital (back-bonding interaction) and a 3 dxz with a $1\pi_g^s$ antibonding orbital of oxygen as shown in Figs 13 and 15. Figure 16

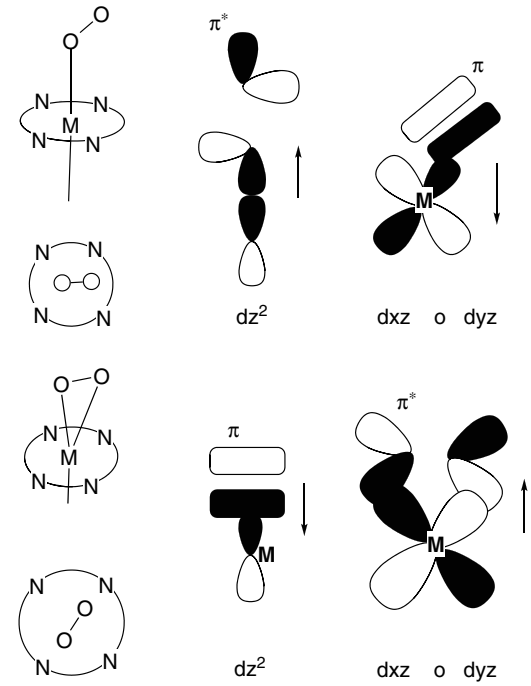

Fig. 13. End-on and side-on interactions of frontier orbitals of O_2 with the frontier orbitals of a metal site. From Ref. [25], reproduced by permission of *The Electrochemical Society Inc*

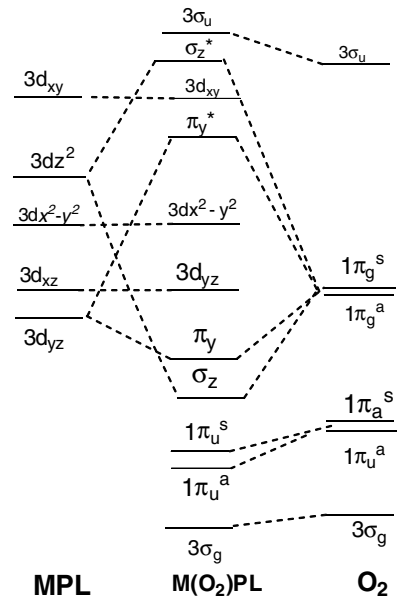

Fig. 14. Qualitative molecular orbital diagram for the end-on $M(O_2)PL$ dioxygen adduct. M=Fe,Co, P=porphyrin, L=NH_3 or imidazole. Reprinted with permission from Ref. [64] *American Chemical Society*

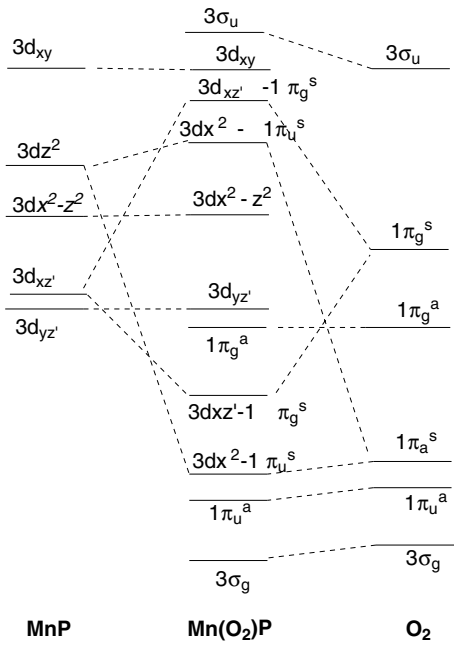

Fig. 15. Qualitative molecular orbital diagram for a side-on $Mn(O_2)PL$ dioxygen adduct. Reprinted with permission from Ref. [64] *American Chemical Society*

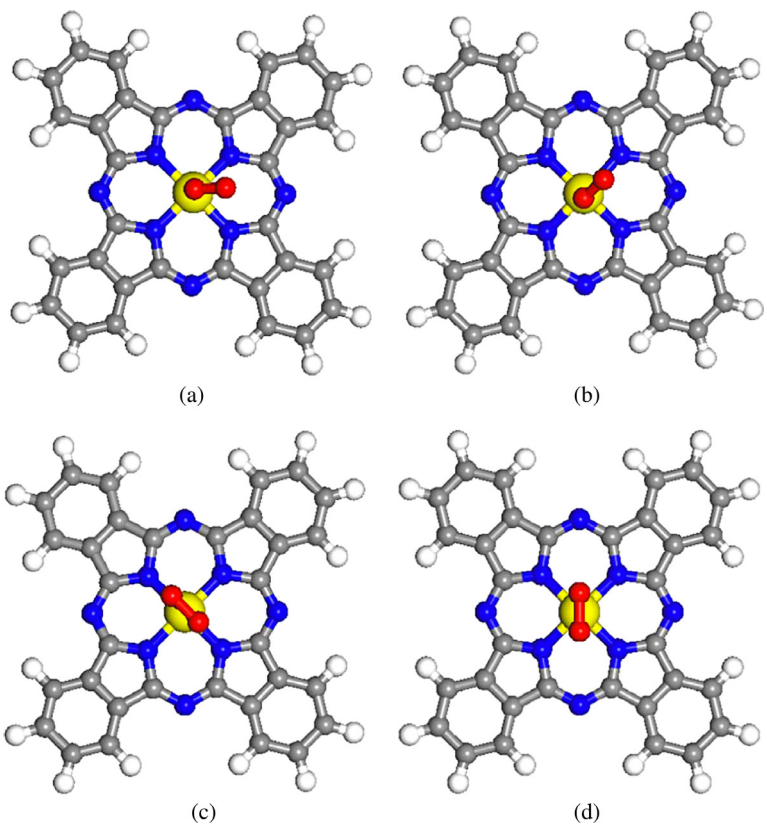

Fig. 16. Optimized structural configurations for the O_2 adsorbed on FePc and CoPc molecules. The upper portion shows two end-on configurations. The lower portion of the figure shows two side-on configurations. The central yellow sphere depicts the metal Fe or Co atom, the central two red spheres represent the adsorbed O_2 molecule, blue spheres represent N atoms, gray spheres represent C atoms and light white spheres represent H atoms. Reproduced with permission from *Taylor and Francis* [65]

illustrates the optimized structural configurations for the O_2 adsorbed on FePc and CoPc molecules according to calculations by Chen *et al.* [64].

The predominating interactions will weaken the O–O bond and increase the O–O distance. The metal in the complex should be in the M(II) state, so for example in alkaline solution a step will require the reduction of M(III):

$$M(III)\text{-}OH + e \leftrightarrows M(II) + OH^-$$

An adduct will be formed according to:

$$M(II) + O_2 \leftrightarrows M(III)\text{-}O_2^- \text{ or } M(II)\text{-}O_2$$

This adduct must be short-lived. Otherwise, it will hinder further O_2 molecules from interacting with the active site. The adduct will undergo reduction as follows:

$$M(III) - O_2^- + e\text{-} \leftrightarrows M(II) + \text{intermediates}$$

where M(II) is the active site. The last reaction shows the process in alkaline media and could involve M(II)–O_2 instead of M(III)–O_2^- especially when Co is the metal center. In acid media the process will involve a proton. The scheme above is applicable to Mn and Fe complexes. In the case of Co complexes, Co(III) is probably not formed upon its interaction with the oxygen molecule since the Co(III)/Co(II) formal potential is much more positive than the M(III)/(II) formal potentials (M= Mn,Fe). However, step 2 is still important since the catalytically active site is Co(II) [53, 65]. Density functional theory calculations [64] have shown that with CoPcs only end-on interaction is possible whereas for FePc both end-on and side-on interactions are plausible. As it will be discussed further, only Mn and Fe phthalocyanines promote the 4-electron reduction of O_2 and this can be attributed to a side-on interaction of O_2, particularly for Fe complexes.

Since the interaction of the oxygen with the active site involves a partial oxidation of the metal in the complex or at least a decrease of electron density in the metal upon interacting with O_2, it is interesting to compare the catalytic activity of metallomacrocyclic with their M(III)/(II) formal potential. Since the formal potentials are sensitive to the pH of the electrolyte, it should be measured in the same media in which the catalytic activity is examined [12, 15, 67]. Further, they should also be measured with the complex adsorbed on the electrode and not in solution phase. When comparing phthalocyanines, the Co and Fe derivatives show the

highest activity for the reduction of O_2 but they behave differently. As pointed out above, Co complexes exhibit Co(III)/(II) transitions that are far more positive than the onset potential for the reduction of O_2 whereas for Fe complexes the onset potential for the catalytic reduction of O_2 is very close to the Fe(III)/(II) transition [12, 53, 65, 67]. For both types of complexes, there is *in situ* spectroscopic evidence for the reversible transition involving the M(III)/(II) couples [65, 68]. For example, for Fe phthalocyanine adsorbed on ordinary pyrolitic graphite, Scherson *et al.* used Fe K-edge XANES (X-ray Absorption Near Edge Structure) recorded *in situ* in 0.5 M H_2SO_4 to prove the evidence for the redox transition of Fe(III)/(II) involving a metal-based orbital.

Many authors have discussed that a correlation should exist between the formal potential of the catalysts and its activity for ORR and it is yet not clear what sort of correlation should be expected. Reduction of O_2 should be observed at the potential of reduction of the M(III) O_2^- adduct and not at the potential of the M(III)/(II) couple. The latter should only be observed if the reaction were outer-sphere, were O_2 would only collide with the redox center without the formation of a bond. In the special case of iron phthalocyanines and other macrocyclics, O_2 reduction usually starts at potentials very close to the Fe(III)/(II) couple [53, 54, 69]. In contrast, for cobalt macrocyclics reduction of O_2 begins at potentials much more negative than those corresponding to the Co(III)/(II) couple [12]. Several authors have reported correlations between activity (measured as potential at constant current) and the M(III)/(II) formal potential and volcano-shaped curves have been obtained [12, 70–72]. This could indicate that the redox potential needs to be located in an appropriate window to achieve maximum activity. In other words, a M(III)/(II) formal potential that is too negative (easily oxidable metal center) or a M(III)/(II) formal potential that is too positive (metal center that is more difficult to oxidize) do not favour the catalysis. However, more recent studies [73–76] have shown that when comparing families of metallophthalocyanines, linear correlations are obtained when plotting log k or log I (rate constant or current at fixed potential) vs. the M(III)/(II) formal potential, as illustrated in Fig. 17. (First order rate constants were calculated as k = I/nAFc, where I is the current at a given potential, n is the total number of electrons transferred, which is 2 for the peroxide pathway and 4 for the reduction to H_2O, A is the area in cm^2, F is the Faraday constant and c is the oxygen concentration in moles per cm^3. What is interesting in the data of Fig. 17 is that one linear correlation is obtained for Cr, Mn and Fe complexes and these metals have configurations d^4(Cr), d^5(Mn) and d^6(Fe). Another linear correlation is obtained for Co complexes, which have a configuration d^7. The other interesting feature in the data of Fig. 17 is that the lines are parallel with a slope close to +0.15 V/decade. It is possible that the declining straight lines in Fig. 17 are part of an incomplete volcano correlation. If so, the slope

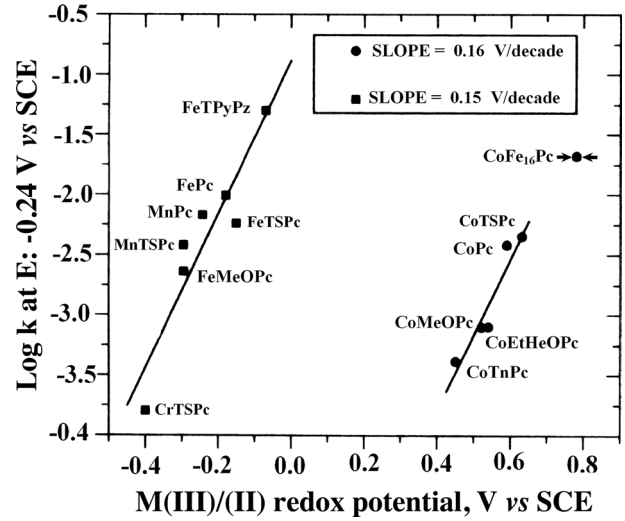

Fig. 17. Plot of log k (at constant potential versus the M(III)/(II) formal potential of the MN4 macrocyclic for the reduction of oxygen in 0.2 M NaOH. From Ref. [75], reproduced by permission of *Elsevier*

0.15 V/decade might have a physical meaning as discussed for the oxidation of thiols [77]. The data in Fig. 17 strongly suggest that more positive redox potentials will increase the catalytic activity. This is important because there seems to be room for improving the catalytic activity of phthalocyanines. The M(III)/(II) redox potential of some macrocyclics can be shifted in the positive direction with heat-treatment. For example when iron tetraphenyl porphyrin [61], FeTPP, is heat-treated, the Fe(III)/(II) redox transition is shifted from 0.2 V *vs.* RHE for fresh FeTPP to 0.4 V for FeTPP heat-treated at 700 °C. Intermediate redox potentials are obtained for heat treatments at intermediate temperatures [61] and the catalytic activity increases with heat treatment, showing that a more positive redox potential of the catalyst favors the O_2 reduction reaction rate. The increase in activity as the M(III)/(II) redox potential of the catalysts is more positive is in contrast to what was previously found in volcano correlations, where a maximum activity is observed for intermediate redox potentials not only for the reduction of O_2 but for other reactions such as the oxidation of thiols or of hydrazine [67]. It is very likely that the data in Fig. 17 corresponds to an incomplete volcano and further studies are necessary to clarify this point using phthalocyanines with extreme positive redox potentials. When studying a series of unsubstituted and substituted Mn phthalocyanines, Nyokong *et al.* [76] have also found that the catalytic activity of these complexes decreases as the Mn(III)/(II) becomes more negative (see Fig. 18) with a slope of 0.24 V/decade. A possible explanation for the results in Fig. 18 (activity decreases as the driving force of the catalyst increases) is that the electronic coupling between the donor (MPc) and the acceptor (O_2) decreases as the electron-donating capacity of the substituents increases, due to a shift in the energy of the

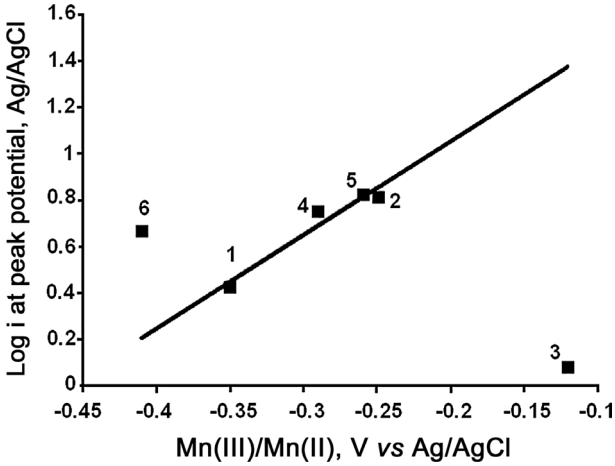

Fig. 18. Plot of log i versus MnIII/MnII redox potential for oxygen reduction in pH 5 buffer. Tebello *et al.* manganese phthalocyanine (MnPc, 1); manganese tetraamino -phthalocyanine (MnTAPc, 2); manganese tetrapentoxy pyrrole phthalocyanine (MnTPePyrPc, 3); manganese tetra phenoxy pyrrole phthalocyanine (MnTPPyrPc, 4); manganese tetra mercaptopyrimidine phthalocyanine (MnTMPyPc, 5) and manganese tetra ethoxy thiophene phthalocyanine (MnTETPc, 6). Taken from Ref. [76] with permission from *Elsevier*

frontier orbitals of the metallophthalocyanine [78–80]. The shift in the energy of the frontier orbital with substituents on cobalt phthalocyanines has been calculated by Schlettwein [78] and Cárdenas-Jirón [81] using PM3 and ZINDO/S semi-empirical theoretical calculations. There are several approaches to estimate the electronic coupling matrix elements between the donor and the acceptor in electron transfer reactions. One of them considers the energy difference between the LUMO (lowest unoccupied molecular orbital) of the electron acceptor and the HOMO (highest occupied molecular orbital) of the electron donor [82] but this requires to know the distance that separates the donor from the acceptor. This is not simple for an inner sphere reaction where the M…O_2 distance could vary from complex to complex. To avoid this difficulty, another reactivity index can be used to explain the data in Fig. 17 and this is the concept of molecular hardness which is a commonly used criterion of reactivity in organic reactions as proposed by Pearson [83]. The hardness η of a single molecule is approximately one-half the energy gap of the HOMO–LUMO, so the larger the gap the greater the hardness the more stable the molecule (the harder the molecule the less its reactivity). The opposite corresponds to a molecule with a narrow HOMO–LUMO gap (soft molecule) situation that will correspond to a very reactive molecule. Now for a donor acceptor pair, it is more convenient to use the concept of donor–acceptor hardness ηDA which is one-half the difference between the energy of the LUMO of the acceptor (O_2 molecule) and the energy of the HOMO of the donor (metal complex).

$$\eta_{DA} = \tfrac{1}{2}(\varepsilon_{LUMOacceptor} - \varepsilon_{HOMOdonor})$$

The donor-acceptor intermolecular hardness can also be described as one-half the difference between the ionization potential of the donor and the electron affinity of the acceptor.

$$\eta_{DA} = -\tfrac{1}{2}(I_{donor} - A_{acceptor})$$

For a gas phase reaction involving the transfer of a single electron, this will be equivalent to the Gibbs free energy of the process ΔGº.

For the special case of Co-phthalocyanine in its ground state, the HOMO is occupied with a single electron (doublet state) so it corresponds to a single occupied molecular orbital (SOMO). The same is valid for molecular oxygen, which in its ground state has two unpaired electrons in two degenerate π* anti-bonding orbitals. In this case, the formation of an adduct CoPc···O_2 involves the interaction of two SOMOs and η_{DA} is given by:

$$\eta_{DA} = \tfrac{1}{2}(\varepsilon_{SOMO/acceptor} - \varepsilon_{SOMO/donor})$$

Figure 19 illustrates the calculated energy levels of the SOMOs of the different cobalt phthalocyanines with respect to the SOMO of oxygen using PM3. Electron-withdrawing substituents (sulfonate, fluoro) on the phthalocyanine ring stabilize the SOMO and the opposite is true for electron-donating groups (methoxy and neopentoxy). So electron-withdrawing groups, even though they decrease the electron density on the cobalt (more positive redox potential) they also decrease the gap between the energy of the SOMO of the phthalocyanine

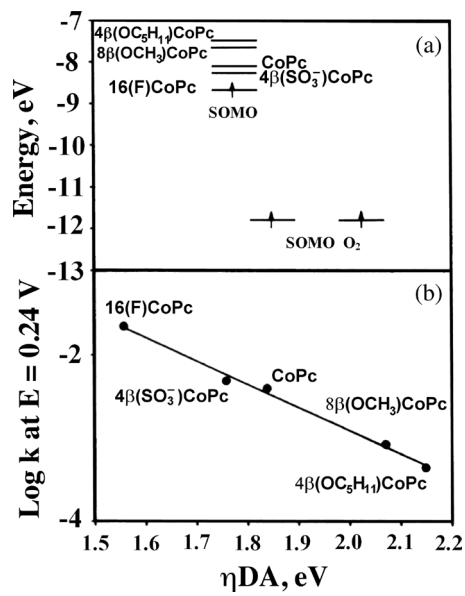

Fig. 19. (a) Relative energies of frontier orbitals of dioxygen and substituted Co phthalocyanines. For simplicity, only one electron is shown on the SOMO of the CoPcs. (b) Plot of log k (at constant potential) versus the donor-acceptor intermolecular hardness for the different O_2–CoPc pairs. From Refs [81, 84], reproduced by permission of *Elsevier*

and the energy of the SOMO of oxygen. The bottom of Fig. 19 shows that log k for O_2 reduction increases as the chemical hardness of the system decreases, or as the softness of the system increases (more reactivity). The trend in reactivity is exactly the same as that illustrated in Fig. 17. It can be concluded then that hardness could be used as a criterion for reactivity of these systems when comparing complexes that bear the same structure, and could explain why, for example perfluorinated phthalocyanine, which has the most positive redox potential (the most oxidant) is the best catalyst for O_2 reduction in the series of cobalt phthalocyanines examined.

Quantum theories of elementary heterogeneous electron transfer (ET) reactions in polar media have been extended to reactions which proceed through active intermediate electronic surface band states or bands. On the basis of this theoretical framework, Ulstrup [85] has interpreted experimental data obtained for O_2 reduction catalyzed by metal phthalocyanines. When comparing activities of complexes by plotting current at a constant potential *vs*. redox potential of the catalyst, linear correlations are also obtained (see Fig. 20) and this was predicted theoretically by the work of Ulstrup [85]. The slope of the lines in Fig. 16 is less than one and this is also predicted by Ulstrup and is attributed to the excitation of intramolecular modes of relatively low frequencies in the cathodic range. The data shown in Fig. 20 is essentially similar to that shown in Fig. 17 but the comparison is made at constant current. So essentially, the graph of Fig. 20 is a plot of driving force versus driving force. This carries the assumption that the M(III)/(II) redox potential provides a measure of the driving force of the catalysts but this might not necessarily be true for inner sphere reactions.

Not all metals of the first transition series exhibit the M(III)/(II) processes, so, if one compares macrocyclics

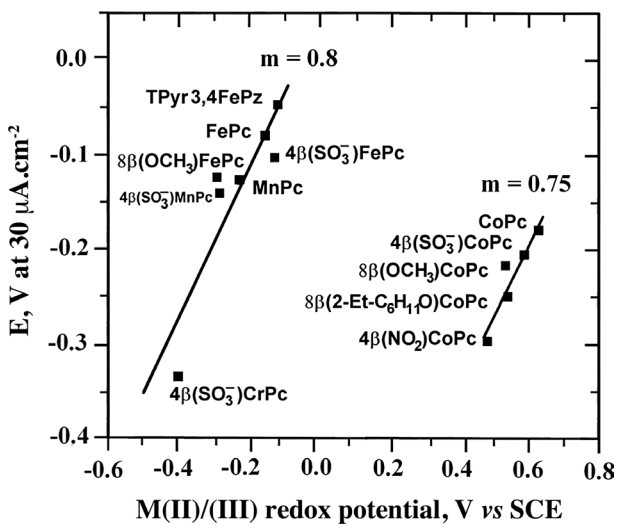

Fig. 20. Plot of E (at constant current) versus the M(III)/(II) formal potential of the MN_4 macrocyclic for the reduction of oxygen in 0.2 M NaOH. From Ref. [75], reproduced by permission of *Elsevier*

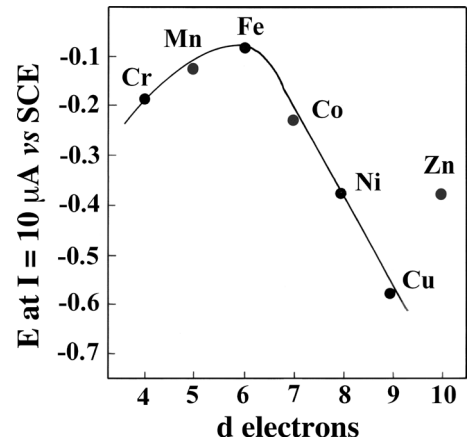

Fig. 21. Volcano plot for the electrocatalytic activity of different M-tetrasulfonated phthalocynaines adsorbed on graphite for O_2 reduction in 0.1 M NaOH, as a function of the number of d-electrons in the metal. From Ref. [53], reproduced by permission of *Elsevier*

of different metals it is convenient to use another parameter, for example the number of d electrons in the metal as shown in Fig. 21. In this Figure, since different Tafel slopes are obtained for the different catalysts, it is not simple to compare activities as current at constant potential. So instead, as a criterion of activity, potential at constant currents is used. It can be clearly seen from Fig. 21 that Fe derivatives exhibit the highest activity, followed by Mn and Co and also illustrates a common observation in catalysis that metals with nearly half filled d-energy levels exhibit the highest activity. So a redox type of mechanism does not operate for metals that do not exhibit the M(III)/(II) transition in the potential window examined for O_2 reduction. This is the case for Ni, Cu and Zn phthalocyanines. It is important to point out that in order to have catalytic activity, the frontier orbital of the $M–N_4$ needs to have some d character as illustrated in Fig. 13. The catalysts with higher activity included in Fig. 19 (Cr, Mn, Fe, Co) have frontier orbitals with d character whereas Ni and Cu phthalocyanines, the frontier orbitals have more ligand character [86] This is illustrated in Fig. 22 [75] that compares the frontier orbitals of CoPc and CuPc. CoPc shows a well-defined dz^2 orbital sticking

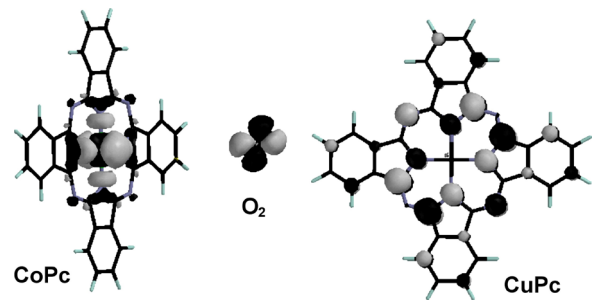

Fig. 22. Illustration of the frontier orbitals involved in the interaction of cobalt phthalocyanine with O_2. Reprinted from Ref. [75] with permission from *Elsevier*

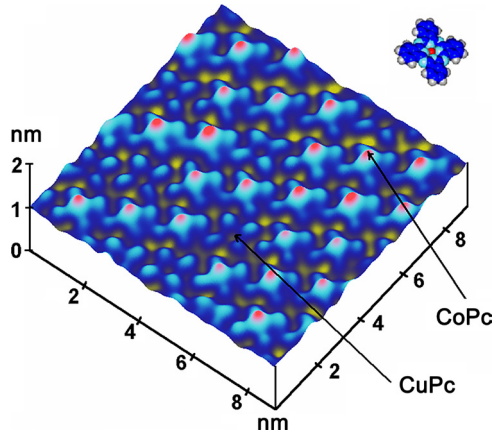

Fig. 23. STM surface plot image of CoPc and CuPc co-adsorbed on the (111) plane of Au. Reprinted with permission from Ref. [87] *American Chemical Society*

out of the plane of the phthalocyanine whereas CuPc does not and shows low activity for O_2 reduction. There is experimental evidence to support this using tunneling electron microscopy. It has shown a strong d-orbital dependence on the images of metal phthalocyanines (see Fig. 23). Unlike copper phthalocyanine where the metal appears as a hole in the molecular image, cobalt phthalocyanine shows the highest point in the molecular image [87]. The benzene regions of CoPc and CuPc show the same height. So, essentially the data using images generated using electron tunneling microscopy is in agreement with the images generated by theoretical calculations.

Even though most authors agree that the M(II) state is the active site for O_2 reduction [15, 54, 59, 65–67, 70, 72, 88, 89] for FePc (iron phthalocyanine) and FeNPc (iron naphthalocyanine) [90, 91]. it has been proposed that Fe(I) could also play a role in the electrocatalytic process. This was based on electroreflectance experiments that indicated that Fe(I) interacts with O_2 whereas Fe(II) does not. However, many authors have shown experimental evidence that O_2 reduction commences at potentials much more positive than those corresponding to the Fe(II)/(I) couple [12, 53, 65, 67]. On the contrary, the reduction currents are observed at potentials close to the potential of the Fe(III)/(II) couple, so it seems unlikely that Fe(I) could be the active site. Worse, as shown from rotating ring-disk experiments, Fe(I) only favors the 2 electron reduction in contrast to Fe(II) [53, 59].

The catalytic activity can also depend on the amount of metal complex present on the electrode surface. In general, the amount of catalyst present on the surface is evaluated from cyclic voltammograms, measuring the electrical charge under reversible peaks. This carries the assumption that all adsorbed catalyst gives an electrochemical signal. This might not necessarily be true and there could be a fraction of complexes present on the surface that are electrochemically silent. It is assumed that the "electroactive" adsorbed species are also active for the reduction of O_2.

It has been found that the O_2 reduction currents are directly proportional to the amount of catalyst present [16, 92], when the catalyst is adsorbed on the electrode surface indicating that the reaction is first order in the surface concentration of catalyst. This is not true for cases where the catalyst is incorporated to the surface by vapor deposition or when the catalyst is deposited from solutions and the solvent is completely evaporated [16]. An explanation for these different observations is that when the catalyst is deposited by vapor deposition or from complete evaporation of solutions, multilayers are formed, and the metal active centers are not all completely accessible to the O_2 molecule. Another example of this type of behavior is the case for polymerized multilayers of cobalt tetraamino-phthalocyanines, where it has been demonstrated that only the outermost layer is active for the reduction of O_2 [55, 56]. Scherson *et al.* have reported that when $(FeTMPP)_2O$ is deposited on a porous support, only 30% of the amount deposited is found to be electrochemically active [93]. Anson *et al.* [94] have found that for the case of $CoPc(CN)_{16}$ and $CoPcF_{16}$ that were deposited from solutions where the solvent was completely evaporated, again it was found that only 30% of the amount deposited was electrochemically active. It was concluded that only those molecules that are directly exposed to the electrolyte and to the incoming O_2 molecules and at the same time are in electric contact with the electrode are active for the reduction of O_2. These results are not surprising since when multilayers are deposited, not all are necessarily in electrical contact with the electrode, which is not the case for adsorbed layers, where molecules are probably lying flat on the electrode surface, interacting with the π system of the graphitic planes. Van der Putten *et al.* [95] have observed catalytic activity with vacuum deposited layers in spite of the fact that these layers are electrochemically silent. As pointed out before when multilayers of metal phthalocyanines are deposited on an electrode surface, only the outermost layer is active for the reduction of O_2 [95] and this is also true for other electrochemical reactions. This shows that multilayers of phthalocyanines or polymerized multilayers of phthalocyanines are rather compact and the inner layers are not accessible to O_2 molecules [56].

N_4-metallomacrocyclic catalysts for one-electron reduction of O_2. An electrode surface that has no active sites should only promote the outer-sphere one-electron reduction of dioxygen. An example of such a surface is a defect-free electrode surface that exposes the basal plane of graphite [89]. On the basal plane, all carbon atoms are fully coordinated so they cannot bind an oncoming molecule like O_2. On electrodes modified with adsorbed catalysts, to the best of our knowledge, there is only one report that shows evidence for the one-electron reduction of O_2 in alkaline media. A reversible one-electron reduction of O_2 to produce the stable superoxide ion was observed in an aqueous solution of 1 M NaOH. This electro-reduction of O_2 was catalyzed by cobalt(II)

1,2,3,4,8,9,10,11,15,16,17,18,22,23,24,25-hexadecafluoro-29*H*,31*H*-phthalocyanine (abbreviated as $Co^{II}PcF_{16}$) adsorbed on a graphite electrode [96]. What is curious is that $Co^{II}PcF_{16}$ is the most active catalyst for the two-electron reduction of O_2 in the correlations shown in Figs 17, 19 and 20, so it is very surprising that it can promote the one-electron reduction of O_2. The OH^- concentration has a very strong effect on the reduction process. Higher OH^- concentrations could stabilize the superoxide ion [89] but 1 M NaOH might not be concentrated enough to achieve this purpose so it could be interetsing to check this experiment by using electron paramagnetic resonance (EPR) techniques to detect any superoxide formation.

N_4-metallomacrocyclic catalysts for two-and four-electron reduction of O_2. Most mono-nuclear Co macrocyclics catalyze the reduction of dioxygen *via* 2-electrons to give peroxide [19, 53, 65, 67, 88]. The activity of Fe phthalocyanines in general is higher than those of Co phthalocyanines and the opposite is true for porphyrins, which reveals the importance of the nature of the ligand in determining the catalytic activity [64]. The opposite is true for heat-treated materials [97]. Cobalt complexes are more stable than iron complexes and this trend is maintained after heat-treatment [72]. However, iron complexes tend to promote the 4-electron reduction of dioxygen and this will be discussed further on.

Lamy *et al.* [98] and van der Putten *et al.* [99] conducted spectroscopic investigations of polymer-modified electrodes containing CoTSPc using UV-visible differential reflectance spectroscopy and were able to identify Co(III)/Co(II) transition when varying the electrode potential. They used electron spin resonance on Ppy (polypyrrol) and Ppy-CoTSPc electrodes in deoxygenated and oxygen saturated solutions. It was shown that the Co(III)TSPc species is effective in the electroreduction of oxygen and that this species is more stable in oxygen saturated medium than in deoxygenated medium because of its stabilization under the following form: Co(III)..O_2. In the case of the Ppy-CoTSPc film, the polypyrrole matrix undergoes strong interactions with oxygen species, and most likely, with hydrogen peroxide.

Phosphoric acid is one of the electrolytes used in fuel cells although very few studies have focused attention on the activity of metallomacrocyclic complexes in this electrolyte. Vasudevan *et al.* [100] investigated the electrocatalytic activity of cobalt phthalocyanine monomers and polymers with imido and carboxylic group ends. The complexes were mixed with carbon powder and polyethylene powder. The activity of the monomeric compounds was found to be higher than that of polymeric compounds.

However, in recent work, Ponce *et al.*, [101] have shown that when Fe phthalocyanine is anchored on gold *via* self-assembled axial ligands, the electrocatalytic activity for ORR increases (see Fig. 24). The increase in activity seems to be associated with the electron-withdrawing effect of the axial ligand. This will shift the Fe(III)/(II) formal potential in the positive direction which favors the catalysis as shown in Fig. 20.

When the catalytic activity of graphite modified with mixtures of different proportions of FeTSPc and CoTSPc was tested for ORR, it was found that the catalysts acted independently, *i.e.* the amount of peroxide generated was directly proportional to the fraction of CoTSPc present on the electrode surface. FeTSPc did not promote the decomposition or reduction of peroxide generated on sites occupied by CoTSPc. However, the possibility for the Fe centres to form hydrogen peroxide and promote its decomposition cannot be ruled out completely since Fe(II) sites are known for their catalase activity [102]. Indeed for some metal complexes van Veen *et al.* have found that their catalytic activity for peroxide decomposition is directly proportional to their activity for O_2 reduction [103].

Again, as observed with FeTSPc and FePc [49, 58, 104, 105] a pre-wave is observed for the reduction currents and corresponds to the direct 4-electron reduction. In contrast to FeTSPc or FePc, production of peroxide was attributed to reduction of the ligand and not reduction of the metal (Fe(I) formation). For this particular catalyst, it was suggested that dioxygen can bind to the

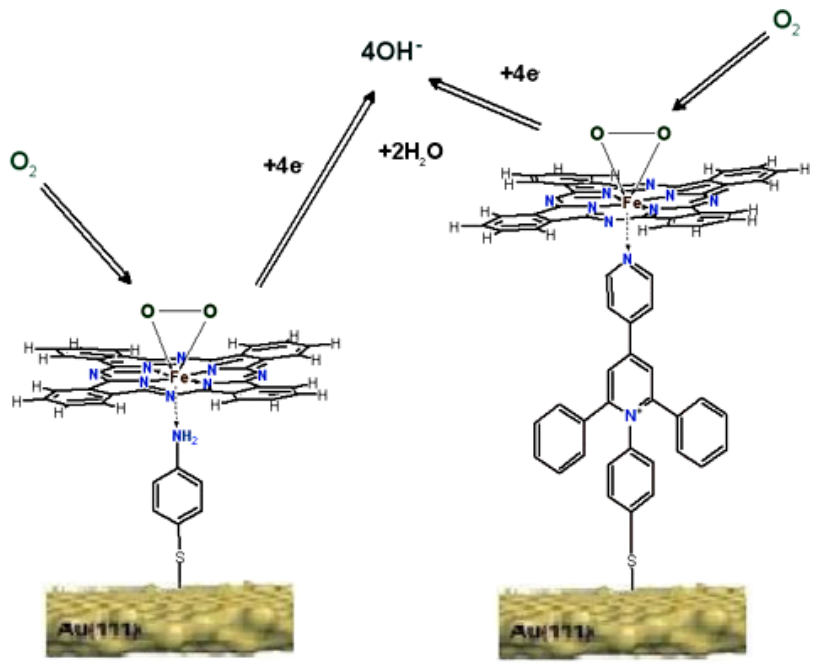

Fig. 24. Illustration of the catalytic action of FePc bound to gold via a self-assembled monolayer of axial ligand bound to Au. Reprinted with permission from Ref. [101] with permission from *Elsevier*

Fe centre and to a highly electronegative nitrogen in the ring, which will avoid the desorption of peroxide before it is reduced. This dual site mechanism would aid charge injection *via* backbonding from the macrocycle into antibonding orbitals of O_2 or bound peroxide causing the destabilization and further rupture of the O–O bond [106]. At more negative potentials at which reduction of the ligand takes place, this mechanism becomes inoperative, the O_2 molecule only binds to the Fe center and peroxide can desorb into the solution. In a study involving heat treated FeTPP [107] and deposited into thick layers on glassy carbon, it was found that the amount of hydrogen peroxide decomposed, compared to the amount of oxygen and hydrogen peroxide reduced, was so small that chemical decomposition was ruled out.

Van den Brink *et al.* [105] when using vacuum deposited layers of FePc have found that when examining the catalytic activity of these layers, the first reduction wave scan was very different from subsequent scans, indicating that some reorganization of the deposited layers took place since this phenomenon is not observed on adsorbed layers of FePc. The effect of irreversible changes of FePc when treated under potential load with oxygen is only observed using vacuum deposited multilayers [90]. Léger *et al.* pointed out that the structure of FePc films influences their electrocatalytic activity. XRD studies have shown that non-heat treated FePc is under the α-phase whereas heat-treated FePc is under the β-phase. Surprisingly, the α-phase shows higher activity than the β-phase (see Fig. 25). These authors have also shown using electrochemical quartz crystal microbalance (EQCM) that α-phase FePc probably forms μ-oxo dimers at potentials higher than 700 mV *vs*. RHE. These μ-oxo dimmers are reduced at the same potential than the monomer of α-phase FePc [106].

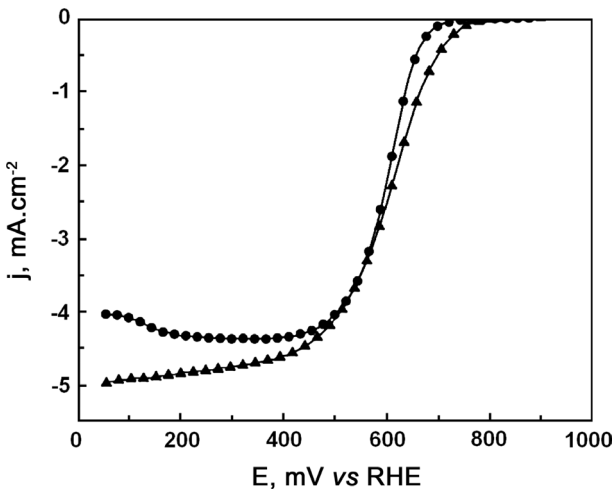

Fig. 25. Polarization curves for the oxygen reduction on a α-FePc/C (m) and a β-FePc (d) disk electrode recorded at 2500 rpm in O_2-saturated 0.5 M H_2SO_4 electrolyte (T = 20 °C, v = 5 mV.s^{-1}). Reprinted from Ref. [106] with the permission of *Elsevier*

Theoretical studies performed by Anderson *et al.* [108] using spin-unrestricted hybrid gradient-corrected density functional calculations have predicted that Fe(II) is the active site for 4-electron reduction of oxygen by iron in the N_4Fe systems employed in the calculation and it may be suggested that the same should be expected for heat-treated iron macrocyclics. The calculations have shown that Fe(II) is favored over Fe(III) because H_2O bonds strongly to the Fe(III) site, preventing O_2 adsorption and water does not bond strongly to Fe(II). On a first step, -OOH bonds more strongly to Fe(II) than to Fe(III), which results in a calculated more reversible potential for its formation over Fe(II). Calculations show that subsequent reduction steps have very reversible potentials over both centers (Fe(II) or Fe(III)). Calculations also show a hydrogen bonding interaction between –(OHOH) bonded to Fe(II) and to a nitrogen lone-pair orbital in the N_4 chelate. This interaction prevents peroxide from desorbing as a two-electron reduction product. So essentially these studies show that adsorbed hydrogen peroxide in an intermediate formed from N_4Fe–OOH on Fe(II) sites and can be released into the solution at more negative potentials as found experimentally [12, 19].

Most catalysts investigated usually have Fe and Co as metal centers. However, complexes of other metals have also been studied. For example CrTSPc and MnTSPc exhibit catalytic activity for ORR [12] and they somehow resemble the behavior of Fe complexes, especially MnTSPc, in the sense that it shows a pre-wave where O_2 reduction proceeds entirely *via* four-electrons to give water. Peroxide is produced at higher polarizations. The lower activity of Cr and Mn phthalocyanines compared to Fe phthalocyanines can be attributed to their low redox potential, *i.e.* they are easily oxidized [53, 72]. The activity of most macrocyclic metal complexes increases after heat treatment [109]. However, the opposite is observed for manganese complexes probably because the metal is lost from the N_4 structure. So, most work dealing with heat-treated materials has focused on Fe and Co macrocycles. Complexes of Mo can only be used in alkaline solution since they are not stable in acid media. MoNPc is less active than FeNPc as reported by Magner *et al.* [110].

Very few authors have studied the effect of temperature [111] on the catalytic activity of phthalocyanines. Baker *et al.*, [111] carried out experiments at different temeperatures in an acidic electrolyte to simulate the environment of an operating PEM fuel cell. They conducted experiments in the temperature range of 20–80 °C and using unsubstituted and substituted Fe phthalocyanines. The surface electrochemical responses of the FePc species were characterized with respect to their surface concentrations and adsorbed surface orientations. Depending on the type of substituent, the adsorption mode could be flat, edge-on, as a dimer, or as an agglomerate, suggesting that the substituent has a strong effect on the FePc species' adsorption mode. Substitution

also has a significant effect on stability. With respect to their electrocatalytic activity, both temperature, substitution and possibly mode of adsorption can significantly affect the ORR mechanism. For example, the overall electron transfer number observed can change from 1 to 3 depending on the type of substituent and the reaction temperature. Further research is required to determine if this change in *n* reflects a change in the ORR pathway, and/or a decrease in the stability of the adsorbed ORR intermediates. Based on the various approaches found in the literature, and the current understanding, a mechanism for the FePc species catalyzed ORR was suggested as follows:

$$FeIIIPc + e- \leftrightarrows FeIIPc \quad (i)$$

$$FeIIPc + O_2 \leftrightarrows O_2\text{–}FeIIPc \quad (ii)$$

$$O_2\text{–}FeIIPc + e- + H+ \leftrightarrows [HO_2\text{–}FeIIIPc] \text{ (r.d. s.)} \quad (iii)$$

$$[HO_2\text{–}FeIIIPc] \rightarrow HO_2^{\bullet -} + FeIIIPc \text{ (hydroperoxyl radical formation)} \quad (iv)$$

$$[HO_2\text{–}FeIIIPc] + e- + 1H^+ \rightarrow H_2O_2 + FeIIIPc \text{ (hydrogen peroxide formation)} \quad (v)$$

$$[HO_2\text{–}FeIIIPc] + 3e- + 3H^+ \rightarrow 2H_2O + FeIIIPc \text{ (water formation)} \quad (vi)$$

It is worth mentioning that Wilkinson *et al.* [112] have also conducted studies at different temperatures using Fe fluoroporphyrin and reported some kinetic parameters such as activation energies. They found that the results were essentially similar to those found with FePc.

CONCLUSION

It can be concluded that in spite of the rather large amount of work published in the literature, there are still many questions that remain unsolved about the electrocatalytic reduction of O_2 mediated by N_4-metallomacrocyclics confined on electrode surfaces. Improving the activity of these complexes beyond the present state-of-the art catalysts will require development of rigorous qualitative and quantitative structure activity relationships (QSAR) [113] for judicious tailoring of activity. Some useful trends do exist. For example, it is now well-established that Fe and Co macrocyclic complexes are by far the best catalysts for oxygen reduction even though some studies have demonstrate that co-facial Ir complexes are also very active. These complexes are characterized by exhibiting a reversible redox transition involving the M(III)/(II) couple. Some authors have found volcano-shaped correlations between activity (measured as current at constant potential or potential at constant current) versus M(III)/(II) formal potential of the catalyst suggesting that an optimal M(III)/(II) redox potential does exist for maximum activity. However, other authors have found only linear correlations between activity and M(III)/(II) redox potential, which indicates that the more positive the redox potential the higher the activity. In the latter correlations, the activity decreases with increasing the driving force of the catalyst. This finding is important since *a priori* one would expect that the more negative the M(III)/(II) formal potential the higher the activity, since this could favour the partial reduction of O_2 upon interacting with the metal centre, *i.e.* M(III)-O_2-. It is also possible that the linear correlations found are part of an incomplete volcano. However, in these correlations it was found that Cr, Mn, Fe and Co complexes, which exhibit a M(III)/(II) transition give rise to two separated correlations or families of compounds. This is a reflection of the fact that the reduction wave for O_2 reduction on for example Mn and Fe complexes starts at a potential very close to the M(III)/(II) formal potential of the catalyst. In contrast, for Co macrocyclics, the reduction wave starts at potentials far more negative than the Co(III)/(II) formal potentials. The proximity of the O_2 reduction wave to the M(III)/(II) for some complexes is also reflected in the observation that a direct four-electron reduction process operates, as observed for Fe and Mn complexes. For most monomeric or monolayers of Co complexes the onset for O_2 reduction is far removed from the Co(III/(II) transition and only the peroxide pathway is observed.

Biomimetic catalyst design schemes have been very successful in tailoring the properties of catalysts, for example, as demonstrated for functional heme/Cu analogs and bimetallic cofacial diporphyrins. The knowledge gained thus far provides a promising leeway for the design of efficient N_4-metallomacrocyclic based catalysts for four-electron reduction of oxygen.

Despite Ir and Ru based N_4-metallomacrocyclic complexes reporting some of the best activities in acidic and alkaline media respectively, being rare metals, their advantageous superiority would be offset by their high cost. Nonetheless, these complexes should serve as appropriate models, such that theoretical and experimental knowledge gained from studying them may serve to tailor the synthesis of improved catalysts. Particularly, the energetic aspects that furnish some monomeric complexes the unique ability to reduce oxygen directly to water as opposed to other monomeric complexes warrant detailed investigation.

The relative back donating power of metal ions attached to the pendant groups of the multinuclear oxygen reduction catalysts discussed in this work is the fundamental parameter for modulating the ORR activity of these complexes. It is therefore possible that the electronic effects introduced due to π-backdonation by Ru(II) and Os(II) may also be fulfilled by other groups. This rationale constitutes the prospect for modulation of the ORR activity of these complexes.

The stability of metalloporphyrins and metallophthalocyanines alike is far from satisfactory for any practical application. Whereas, there is irrefutable evidence for improved activity upon heat treatment of the

N_4-metallomacrocyclic complexes, the loss of their structural merit is obvious. The fact that the performance of non-precious metal catalysts synthesized by heat treatment of inexpensive nitrogen, carbon and metal precursors rivals that of heat treated N_4-metallomacrocyclic complexes, which are relatively more expensive, renders the latter to be non-competitive precursors. [114]. On the other hand, improving the stability and activity of N_4-metallomacrocyclic complexes while conserving their molecular integrity is a difficult task, and indeed very little progress has been reported in line with this.

New material design approaches including exploitation of the synergetic benefits reported for some catalyst supports, for example, carbon nanotubes, graphene, nitrogen doped carbons and titania [115], and conductive mesoporous materials with high surface areas, among others, might help to solve some of the current challenges. The multicomponent and multifunctional approach where the individual components of a composite catalyst perform specific reactions to ensure complete reduction of oxygen is worthwhile engendering.

Finally, it is worth mentioning that some of the advantages of $M–N_4$ macrocyclics over Pt catalysts is their tolerance to methanol crossover, which is a serious problem in methanol-air fuel cells [17]. For example Léger *et al.* have shown that FePc is highly tolerant to methanol [116]. The same is true for CoPc [117]. When methanol crossover from the anode through the electrolytic membrane to the cathode occurs, electroreduction of dioxygen and electrooxidation of methanol occur simultaneously. Such an incidence would be detrimental to the overall performance of the fuel cell since the fuel efficiency decreases and so does the power output. In general $M–N_4$ macrocyclics are poor catalysts for the oxidation of methanol so this reaction should not occur and this would avoid the problems mentioned above.

Acknowledgements

J.H. Zagal is grateful to Fondecyt 1100773 and Núcleo Milenio Project P07-006 Iniciativa Científica Milenio del Ministerio de Economía, Fomento y Turismo for financial support. Justus Masa is grateful to the German Academic Exchange Service (DAAD) for a PhD scholarship.

ABBREVIATIONS

pCoTTP	poly{[*meso*-tetrakis(thienyl)porphyrinato] cobalt(II)}
Co_2FTF_4	dicobalt "face-to-face" diporphyrin with a four atom amide bridge
TSPc	tetrasulphophthalocyanine
TcPc	tetracarboxyphthalocyanine
OcPc	octacarboxyphthalocyanine
TPyP	*meso*-tetrakis(4-pyridyl)porphyrin
RuOCPcPt	Ruthenium tetrakis-(diaquaplatinum)octacarboxy phthalocyanine
OEP	2,3,7,8,12,13,17,18-octaethylporphyrin
TMeP	*meso*-tetramethyl porphyrin
CoP	Cobalt porphine
FeOCPcPt	Iron tetrakis(diaquaplatinum)octacarboxyphthalocyanine
CoPIX	Cobalt protoporphyrin
CcO	Cyctochrome c oxidase

REFERENCES

1. Steele BC and Heinzel A. *Nature*. 2001; **414**: 345–352.
2. Spendelow JS and Wieckowski A. *Phys. Chem. Chem. Phys*. 2007; **9**: 2654–2675.
3. Lee J, Kim ST, Cao R, Choi N, Liu M, Lee KT and Cho J. *Adv. Energ. Mater.* 2011; **1**: 34–50.
4. Ramamoorthy R, Dutta PK and Akbar SA. *J. Mater. Sci.* 2003; **38**: 4271–4282.
5. Gasteiger HA, Kocha SS, Sompalli B and Wagner FT. *Appl. Catal., B*. 2005; **56**: 9–35.
6. a) Min M. *Electrochim. Acta*. 2000; **45**: 4211–4217. b) Mazumder V, Lee Y and Sun S. *Adv. Funct. Mater.* 2010; **20**: 1224–1231. c) Sun Z, Masa J, Liu Z, Schuhmann W and Muhler M. *Chem. Eur. J.,* 2012; doi: 10.1002/chem.201103253.
7. http://www.platinum.matthey.com/pgm-prices/; accessed on February 27, 2012.
8. Jasinski R. *Nature*. 1964; **201**: 1212–1213.
9. a) H. Jahnke, M. Schönborn and G. Zimmermann. *Top. Curr. Chem*., 1976; **61**: 133–181. b) Alt H, *J. Catal.* 1973; **28**: 8–19.
10. Kadish K. *J. Electroanal. Chem.* 1984; **168**: 261–274.
11. a) Randin J. *Electrochim. Acta*. 1974; **19**: 83–85. b) Richards G and Swavey S. *Eur. J. Inorg. Chem.* 2009: 5367–5376.
12. Zagal J, Páez M, Tanaka A, dos Santos J and Linkous C. *J. Electroanal. Chem.* 1992; **339**: 13–30.
13. Yuasa M, Nishihara R, Shi C and Anson FC. *Polym. Adv. Technol.* 2001; **12**: 266–270.
14. a) Song E, Shi C and Anson FC. *Langmuir*. 1998; **14**: 4315–4321. b) Ozer D, Harth R, Mor U and Bettelheim A. *J. Electroanal. Chem.* 1989; **266**: 109–123. c) Bettelheim A, Ozer D, Harth R and Murray RW. *J. Electroanal. Chem.* 1989; **266**: 93–108.
15. van der Putten A, Elzing A, Visscher W and Barendrecht E. *J. Electroanal. Chem.* 1987; **221**: 95–104.
16. Elzing A, van der Putten A, Visscher W and Barendrecht E. *J. Electroanal. Chem.* 1986; **200**: 313–322.
17. Radoslav Adzic. In *Electrocatalysis*. *Recent Advances in Kinetics of Oxygen Reduction*, Lipkowski J and Ross PN. (Ed.) Wiley-VCH: New York, 1998; pp 197–237.
18. Bard AJ and Faulkner LR. *Electrochemical Methods. Fundamentals and Applications*, (2nd Edn.) Wiley: New York 2001.
19. Zagal J. *J. Electrochem. Soc*. 1980; **127**: 1506.

20. Paulus UA, Schmidt TJ, Gasteiger HA and Behm RJ. *J. Electroanal. Chem.* 2001; **495**: 134–145.
21. Dobrzeniecka A, Zeradjanin A, Masa J, Puschhof A, Stroka J, Kulesza PJ and Schuhmann W. *Catal. Today*, doi: 10.1016/j.cattod.2012.03.060.
22. Kim E, Chufán EE, Kamaraj K and Karlin KD. *Chem. Rev*. 2004; **104**: 1077–1134.
23. Collman JP and Ghosh S. *Inorg. Chem.* 2010; **49**: 5798–5810.
24. a) Collman JP, Boulatov R, Sunderland CJ and Fu L. *Chem. Rev*. 2004; **104**: 561–588. b) Collman JP, Devaraj NK, Decreau RA, Yang Y, Yan Y, Ebina W, Eberspacher TA and Chidsey CED. *Science* 2007; **315**: 1565–1568.
25. Boulatov R, Collman JP, Shiryaeva IM and Sunderland CJ. *J. Am. Chem. Soc*. 2002; **124**: 11923–11935.
26. Chang CJ, Deng YQ, Shi CN, Chang CK, Anson FC and Nocera DG. *Chem. Commun*. 2000: 1355–1356.
27. Collman JP. *Science*. 1997; **275**: 949–951.
28. Collman JP, Denisevich P, Konai Y, Marrocco M, Koval C and Anson FC. *J. Am. Chem. Soc*. 1980; **102**: 6027–6036.
29. Shigehara K and Anson FC. *J. Phys. Chem*. 1982; **86**: 2776–2783.
30. Collman JP, Elliott CM, Halbert TR and Tovrog BS. *Proc. Natl. Acad. Sci. U. S. A*. 1977; **74**: 18–22.
31. Chang CK, Liu HY and Abdalmuhdi I. *J. Am. Chem. Soc.* 1984; **106**: 2725–2726.
32. Liu HY, Abdalmuhdi I, Chang CK and Anson FC. *J. Phys. Chem*. 1985; **89**: 665–670.
33. Collman JP, Wagenknecht PS and Hutchison JE. *Angew. Chem. Int. Ed*. 1994; **33**: 1537–1554.
34. Durand RR, Bencosme CS, Collman JP and Anson FC. *J. Am. Chem. Soc.* 1983; **105**: 2710–2718.
35. Anson FC, Shi C and Steiger B. *Acc. Chem. Res*. 1997; **30**: 437–444.
36. Collman JP, Hendricks NH, Kim K and Bencosme CS, *J. Chem. Soc., Chem. Commun*. 1987: 1537.
37. Chang CJ, Loh Z, Shi C, Anson FC and Nocera DG. *J. Am. Chem. Soc.* 2004; **126**: 10013–10020.
38. Collman JP and Kim K. *J. Am. Chem. Soc.* 1986; **108**: 7847–7849.
39. Collman JP, Chng LL and Tyvoll DA. *Inorg. Chem.* 1995; **34**: 1311–1324.
40. Shi C, Mak KW, Chan KS and Anson FC. *J. Electroanal. Chem.* 1995; **397**: 321–324.
41. Bouwkamp-Wijnoltz AL, Visscher W and van Veen J. *Electrochim. Acta*. 1994; **39**: 1641–1645.
42. Shi C, Steiger B, Yuasa M and Anson FC. *Inorg. Chem.* 1997; **36**: 4294–4295.
43. Shi C and Anson FC. *Inorg. Chem.* 1992; **31**: 5078–5083.
44. a) Steiger B and Anson FC. *Inorg. Chem.* 1997; **36**: 4138–4140. b) Shi C and Anson FC. *Inorg. Chem.* 1996; **35**: 7928–7931.
45. Shi C and Anson FC. *J. Am. Chem. Soc.* 1991; **113**: 9564–9570.
46. Maxakato NW, Mamuru SA and Ozoemena KI. *Electroanalysis*. 2011; **23**: 325–329.
47. a) Mamuru SA and Ozoemena KI. *Electrochem. Commun.* 2010; **12**: 1539–1542. b) Mamuru SA, Ozoemena KI, Fukuda T and Kobayashi N. *J. Mater. Chem*. 2010; **20**: 10705.
48. Chen R, Li H, Chu D and Wang G. *J. Phys. Chem. C*. 2009; **113**: 20689–20697.
49. Zagal JH, Páez M, Sturn J and Ureta-Zañartu S. *J. Electroanal. Chem.* 1984; **181**: 295–300.
50. Dobrzeniecka A, Zeradjanin A, Masa J, Stroka J, Goral M, Schuhmann W and Kulesza PJ. *ECS Trans*. 2011; 35: 33–44.
51. Forshey PA and Kuwana T. *Inorg. Chem.* 1983; **22**: 699–707.
52. Zagal JH. *Macrocycles,* In *Handbook of Fuel Cells-Fundamentals, Technology and Applications*, Vol. 2, Part 5, John Wiley & Sons, Ltd.: Chichester, 2003; 544.
53. Zagal JH. *Coord. Chem. Rev.* 1992; **119**: 89–136.
54. Zagal JH and Bedioui F. *N_4-Macrocyclic Metal Complexes*, Springer: New York, 2006.
55. Tse Y, Janda P, Lam H, Zhang J, Pietro WJ and Lever A. *J. Porphyrins Phthalocyanines* 1997; **1**: 3–16.
56. Pavez J, Paez M, Ringuede A, Bedioui F and Zagal JH. *J Solid State Electrochem*. 2005; **9**: 21–29.
57. Ramírez G, Trollund E, Isaacs M, Armijo F, Zagal J, Costamagna J and Aguirre M. *Electroanalysis*. 2002; **14**: 540–545.
58. Lalande G, Cote R, Guay D, Dodelet JP, Weng LT and Bertrand P. *Electrochim. Acta*. 1997; **42**: 1379–1388.
59. Bouwkamp-Wijnoltz A, Visscher W and van Veen J. *Electrochim. Acta*. 1998; **43**: 3141–3152.
60. a) Lefevre M, Dodelet JP and Bertrand P. *J. Phys. Chem. B*. 2002; **106**: 8705–8713. b) Lefèvre M. *Electrochim. Acta*. 2003; **48**: 2749–2760. c) Schilling T, Okunola A, Masa J, Schuhmann W and Bron M. *Electrochim. Acta*. 2010; **55**: 7597–7602.
61. Bouwkamp-Wijnoltz AL, Visscher W, van Veen JA, Boellaard E, van der Kraan and Tang SC. *J. Phys. Chem. B*. 2002; **106**: 12993–13001.
62. Kobayashi N and Nevin WA. *Appl. Organomet. Chem.* 1996; **10**: 579–590.
63. Bytheway I and Hall MB. *Chem. Rev*. 1994; **94**: 639–658.
64. Wang G, Ramesh N, Hsu A, Chu D and Chen R. *Mol. Simul.* 2008; **34**: 1051–1056.
65. *Transition Metal Macrocycles as Electrocatalysts for Dioxygen Reduction*, In Electrochemical Surface Modification: *Thin Films, Functionalization and Characterization*, Scherson DA, Palencsr A, Tolmachev Y and Stefan I. (Eds.) Wiley-VCH Verlag GmbH & Co. KGaA: Weinheim, Germany, 2008.
66. Zecevic S, Simic-Glavaski B, Yeager E, Lever A and Minor P. *J. Electroanal. Chem.* 1985; **196**: 339–358.

67. Zagal JH, Griveau S, Francisco Silva J, Nyokong T and Bedioui F. *Coord. Chem. Rev.* 2010; **254**: 2755–2791.
68. a) Kim S and Scherson DA. *Anal. Chem*. 1992; **64**: 3091–3095. b) Stefan IC, Mo Y, Ha SY, Kim S and Scherson DA. *Inorg. Chem.* 2003; **42**: 4316–4321.
69. Wiesener K, Ohms D, Neumann V and Franke R. *Mater. Chem. Phys.* 1989; **22**: 457–475.
70. Vasudevan P, Santosh, Mann N and Tyagi S. *Transition Met Chem*. 1990; **15**: 81–90.
71. van Veen J. *Electrochim. Acta*. 1979; **24**: 921–928.
72. Vanveen JA, VanBaar JF, Kroese CJ, Coolegem JG, Dewit N and Collin HA. *Berichte der Bunsen-Gesellshaft-Physical Chemistry Chemical Physics* 1981; **85**: 693–700.
73. Zagal JH, Aguirre MJ, Basaez, Pavez J, Padilla L and Toro-Labbé A. *The Electrochemical Society Symposium Series.* 1995; **89**: 95–26.
74. Zagal JH, Gulppi M, Isaacs M, Cardenas-Jiron G and Aguirre MJ. *Electrochim. Acta*. 1998; **44**: 1349–1357.
75. Cardenas-Jiron GI, Gulppi MA, Caro CA, del Rio R, Paez M and Zagal JH. *Electrochim. Acta*. 2001; **46**: 3227–3235.
76. Sehlotho N and Nyokong T. *J. Electroanal. Chem.* 2006; **595**: 161–167.
77. Bedioui F, Griveau S, Nyokong T, John Appleby A, Caro CA, Gulppi M, Ochoa G and Zagal JH. *Phys. Chem. Chem. Phys*. 2007; **9**: 3383.
78. Schlettwein D and Yoshida T. *J. Electroanal. Chem.* 1998; **441**: 139–146.
79. Zagal JH and Cardenas-Jiron GI. *J. Electroanal. Chem.* 2000; **489**: 96–100.
80. Cardenas-Jiron GI and Zagal JH. *J. Electroanal. Chem.* 2001; **497**: 55–60.
81. Zagal JH, Gulppi MA and Cárdenas-Jirón G. *Polyhedron*. 2000; **19**: 2255–2260.
82. Newton MD. *Chem. Rev*. 1991; **91**: 767–792.
83. a) Pearson RG. *Proc. Natl. Acad. Sci. U. S. A*. 1986; **83**: 8440–8441. b) Parr RG and Pearson RG. *J. Am. Chem. Soc.* 1983; **105**: 7512–7516.
84. Zagal JH and Cárdenas-Jirón GI. *J. Electroanal. Chem.* 2000; **489**: 96–100.
85. Ulstrup J. *J. Electroanal. Chem.* 1977; **79**: 191–197.
86. Rosa A and Baerends EJ. *Inorg. Chem.* 1994; **33**: 584–595.
87. Hipps KW, Lu X, Wang XD and Mazur U. *J. Phys. Chem*. 1996; **100**: 11207–11210.
88. Jasinski R. *J. Electrochem. Soc*. 1965; **112**: 526.
89. Yeager E. *Electrochim. Acta*. 1984; **29**: 1527–1537.
90. Hinnen C, Coowar F and Savy M. *J. Electroanal. Chem.* 1989; **264**: 167–180.
91. a) van den Ham D, Hinnen C, Magner G and Savy M. *J. Phys. Chem*. 1987; **91**: 4743–4748. b) Coowar F, Contamin O, Savy M and Scarbeck G. *J. Electroanal. Chem.* 1988; **246**: 119–138.
92. Elzing A, van der Putten A, Visscher W and Barendrecht E. *J. Electroanal. Chem.* 1987; **233**: 99–112.
93. Fierro CA, Mohan M and Scherson DA. *Langmuir*. 1990; **6**: 1338–1342.
94. Ouyang J, Shigehara K, Yamada A and Anson FC. *J. Electroanal. Chem.* 1991; **297**: 489–498.
95. van der Putten A, Elzing A, Visscher W and Barendrecht E. *J. Electroanal. Chem.* 1986; **214**: 523–533.
96. Song C, Zhang L and Zhang J. *J. Electroanal. Chem.* 2006; **587**: 293–298.
97. Kalvelage H, Mecklenburg A, Kunz U and Hoffmann U. *Chem. Eng. Technol.* 2000; **23**: 803–807.
98. Coutanceau C, Rakotondrainibe A, Crouigneau P, Léger J and Lamy C. *J. Electroanal. Chem.* 1995; **386**: 173–182.
99. Elzing A, van der Putten A, Visscher W, Barendrecht E and Hinnen C. *J. Electroanal. Chem.* 1990; **279**: 137–156.
100. Phougat N and Vasudevan P. *J. Power Sources*. 1997; **69**: 161–163.
101. Ponce I, Silva JF, Oñate R, Rezende MC, Páez MA, Pavez J and Zagal JH. *Electrochem. Commun*. 2011; **13**: 1182–1185.
102. Sheldon RA and Kochi JK. *Metal-catalyzed oxidations of organic compounds*, Academic Press: New York. 1981.
103. van Veen JAR and van Baar. *Rev. Inorg. Chem*. 1982; **4**: 293.
104. Elzing A, van der Putten A, Visscher W and Barendrecht E. *J. Electroanal. Chem.* 1987; **233**: 113–123.
105. van Den Brink F, Visscher W and Barendrecht E. *J. Electroanal. Chem.* 1984; **172**: 301–325.
106. Baranton S, Coutanceau C, Garnier E and Léger J. *J. Electroanal. Chem.* 2006; **590**: 100–110.
107. Ikeda O, Fukuda H and Tamura H. *J. Chem. Soc., Faraday Trans. 1*. 1986; **82**: 1561.
108. Anderson AB and Sidik RA. *J. Phys. Chem. B*. 2004; **108**: 5031–5035.
109. *The porphyrin handbook*, Kadish KM, Smith KM and Guilard R. (Eds.) Academic Press: San Diego, California, London, 2003.
110. Magner G. *J. Electrochem. Soc*. 1981; **128**: 1674.
111. Baker R, Wilkinson D and Zhang J. *Electrochim. Acta*. 2008; **53**: 6906–6919.
112. Zhang L, Song C, Zhang J, Wang H and Wilkinson DP. *J. Electrochem. Soc*. 2005; **152**: A2421.
113. Hu X, Liu C, Wu Y and Zhang Z. *J. Phys. Chem. C*. 2011; **115**: 23913–23921.
114. Masa J, Schilling T, Bron M and Schuhmann W. *Electrochim. Acta*. 2012; **60**: 410–418.
115. a) Xia W, Masa J, Bron M, Schuhmann W and Muhler M. *Electrochem. Commun.* 2011; **13**: 593–596. b) Masa J, Bordoloi A, Muhler M, Schuhmann W and Xia W. *ChemSusChem.* 2012; **5**: 523–525.
116. Baranton S, Coutanceau C, Roux C, Hahn F and Léger J. *J. Electroanal. Chem.* 2005; **577**: 223–234.
117. Lu Y and Reddy R. *Electrochim. Acta*. 2007; **52**: 2562–2569.